GA-A14834
UC-77

ANALYSIS OF FULL CORE STEAM FLOODING EXPERIMENTS FOR THE PHASE II GCFR CRITICAL ASSEMBLY

by
A. L. HESS and R. A. RUCKER

Prepared under
Contract EY-76-C-03-0167
Project Agreement No. 23
for the San Francisco Operations Office
Department of Energy

GENERAL ATOMIC PROJECT 3228
DATE PUBLISHED: MAY 1978

GENERAL ATOMIC COMPANY

ABSTRACT

The initial program of benchmark critical experiments conducted in behalf of the design and safety evaluations for the 300 MW(e) gas cooled fast breeder reactor demonstration plant included extensive measurements of the reactivity effects of accidental steam ingress. Insertions of polyethylene (CH_2) foam into all of the void channels in the 1250-liter (ℓ) core, the radial blankets, and the axial blankets of the Phase II GCFR critical assembly gave simulated floodings of up to 2.25% steam in the coolant. This report presents results of General Atomic Company (GA) analyses of the Phase II steam entry experiments, giving comparisons of calculated and measured flooding worths under various conditions, including changes in core geometry and introduction of control rod poisoning. Also studied were the effects of steam flooding on control material worth and other physics parameters. Calculated worths of hydrogenous materials were found to be significantly sensitive to variations in analytical models and methods. Good agreement with experiments was obtained by a 28-group analysis when a rigorous regeneration of cross-sections, cell-heterogeneity factors, and directional diffusion coefficients was provided at each specific flooding density to account for the moderated spectra. Steam worths in a rodded core can be similarly well predicted provided that rod shielding effects are re-evaluated in the steam environment. Extrapolations based on these experiments clearly suggest that should a steam leak incident occur, it would not be a major safety concern, even in a small GCFR demonstration plant. Details of the analytical procedures and models utilized are presented in this report.

CONTENTS

FIGURES

TABLES

TABLES (continued)

1. INTRODUCTION

Among the questions to be resolved in preparation for licensing the gas-cooled fast reactor (GCFR) is the potential of steam ingress into the core coolant channels resulting from a hypothetical steam line break in the helium/steam heat exchanger. The probable frequency of such accidents, the potential leak rates, and the limiting channel steam densities are among the mechanical hydraulic design aspects of the question which must be considered.

The neutronic aspects include the effects of the resulting steam ingress on the core reactivity and on the capability of the control system to shut down the reactor. These effects have proved sensitive not only to the steam density involved, but also to several features and conditions of the reactor configuration, including core shape, fuel enrichment, control and fission-product poisoning, and fuel temperature.

The development program for the 300 MW(e) GCFR demonstration plant (Ref. 1) project includes several series of critical experiments (Ref. 2) for the verification of core design methodologies. During the initial stage of this critical experiment work, a three-phase series of clean-geometry GCFR assemblies was constructed on the Zero Power Reactor-9 (ZPR9) facility at Argonne National Laboratory (ANL). The experimental programs for these three assemblies, planned jointly by General Atomic Company (GA) and Argonne personnel, included extensive studies of steam worth.

In the Phase I assembly (Ref. 3), with a 3150-ℓ core, the steam-entry studies were limited to scoping experiments in a central 47-ℓ zone. The GA analyses for these worth measurements have been reported by Hess et al. (Ref. 4). In the Phase II assembly (Ref. 5), with a 1300-ℓ core, full core

and blanket steam flooding was simulated. In the follow-on Phase III, to be reported, a three-zone GCFR core was represented and steam worth studies were made in a pin zone environment.

This report presents the results of the GA analysis of the full-core simulated steam flooding experiments carried out in the Phase II assembly. Objectives in the Phase II steam entry studies included:

1. Measuring variations of steam worth with flooding density and core geometry changes.

2. Determining the influence of control poisoning on steam worth.

3. Ascertaining the effect of steam on control rod worths.

4. Investigating the influence of steam on other physics parameters.

These objectives were achieved through a series of loadings for steam flooding, rod insertions, steam removal with rods installed, and withdrawal of the rods in a dry configuration.

The Phase II configuration was generically typical of a demonstration-sized GCFR at power. Although fuel construction, coolant channel geometry, and temperature for the critical experiment differ from an operating GCFR, the steam experiments here have provided a valuable data set for scoping the reactivity effects of steam and testing the methodologies employed at GA for predicting the effects of steam ingress into the coolant of a GCFR.

2. DESCRIPTION OF THE PHASE II GCFR ASSEMBLY

The ZPR9 at Argonne, Illinois is one of several split-table critical-assembly machines in the U.S. and abroad employed for studying the physics characteristics of fast-neutron reactor systems. The halves of the reactor, on the fixed and movable tables, consist of square arrays of steel matrix tubes (45 tubes by 45 tubes), each of which is 5.52 cm square and 122 cm long. Steel trays or drawers, loaded with longitudinal columns of fuel, fertile, and diluent plates, are installed in the matrix tubes in prescribed array patterns to provide the core, blanket, reflector, etc., regions for the fast reactor configuration under study. Although an assembly is operated at low power (1 kW or less), measurements thereon provide essential physics parameters such as critical size, power profiles, reaction-rate profiles, reactivity coefficients, and neutron-spectral indices representative of similarly designed power production reactors.

Figure 1 shows the basic radial outlines of the core, blanket, and reflector regions for the reflected reference configuration of the Phase II GCFR assembly. In each axial half of the reactor the core extends 61.04 cm, the adjacent axial blanket extends 30.48 cm, and the axial reflector extends 15.24 cm beyond the blanket. Also shown are the radial locations for simulated B_4C control rod installations, at the core center and at seven positions in a ring of about a seven drawer radius. The ZPR9 operational shutdown rod positions precluded the loading of the eighth rod of the ring, which would have otherwise provided a symmetric pattern.

Throughout the steam worth program the core outline, and thus volume and effective radius, was changed several times to accommodate reactivity effects of particular experiments by exchanges of core drawers for blanket drawers. The fuel density and enrichment in the core were thus kept constant. For the basic configuration without B_4C rods installed, the critical mass was 589 kg fissile Pu in an effective core volume of 1236 ℓ. With

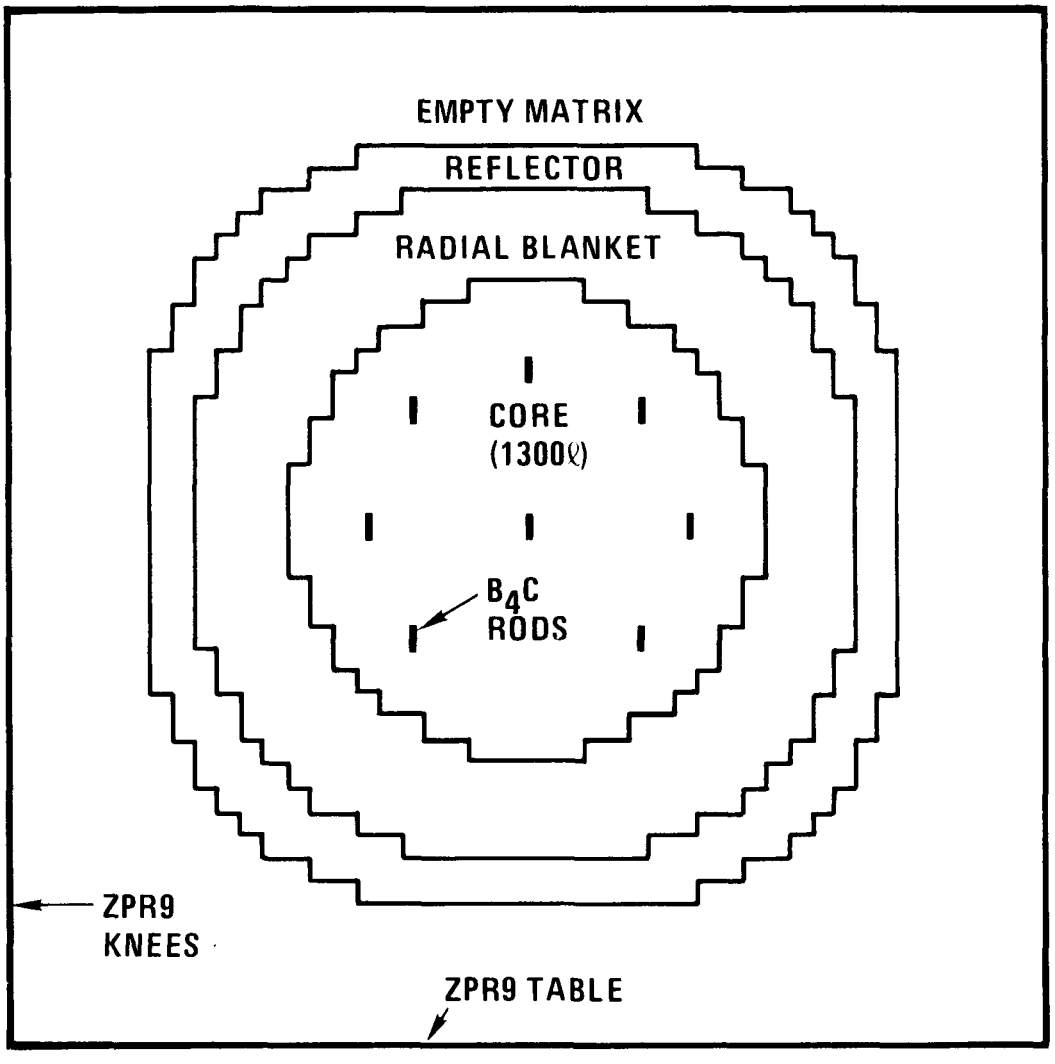

Fig. 1. Midplane view of Phase II GCFR critical assembly during steam worth experiments

eight B_4C rods in place, loading to near critical again required a core expansion to about 1352 ℓ. Extensive details on the Phase II construction have been reported by Pond (Ref. 5).

Figure 2 illustrates the heterogeneous nature of the core loadings for the Phase II assembly. The repeating, three-drawer core unit-cell contained four columns each of Pu-U-Mo alloy (sandwiched between Fe_2O_3 plates) and U_3O_8 for a simulation of mixed-oxide fuel enriched to 17% fissile plutonium. Steam flooding was simulated by inserting slabs of perforated polyethylene foam into the void channels, with the slab density averaging 17.5 g CH_2/ℓ. Intermediate flooding densities were approximated by foam-CH_2 insertions into the void channels of one-half or one-fourth of the core and blanket drawers, using alternating patterns of void and flooded drawers for loading convenience.

Figure 2 also illustrates the calculational model used for the TWOTRAN (Ref. 6) two dimensional discrete ordinate cell calculations to derive shielding factors for the mockup control rod, which consisted of a 1.27 x 5.08-cm (1/2 x 2-in.) column of boron carbide clad in steel. By utilizing a reflective boundary condition on the lower horizontal axis, this scheme represented a 3 x 3 drawer configuration with a central B_4C rod. The standard three-drawer core unit cell can be visualized as the top two-thirds of the figure. As a model for TWOTRAN, the diagram exhibits somewhat less heterogeneity than the true physical cell since the cladding of the fuel and void channels are merged into adjacent regions.

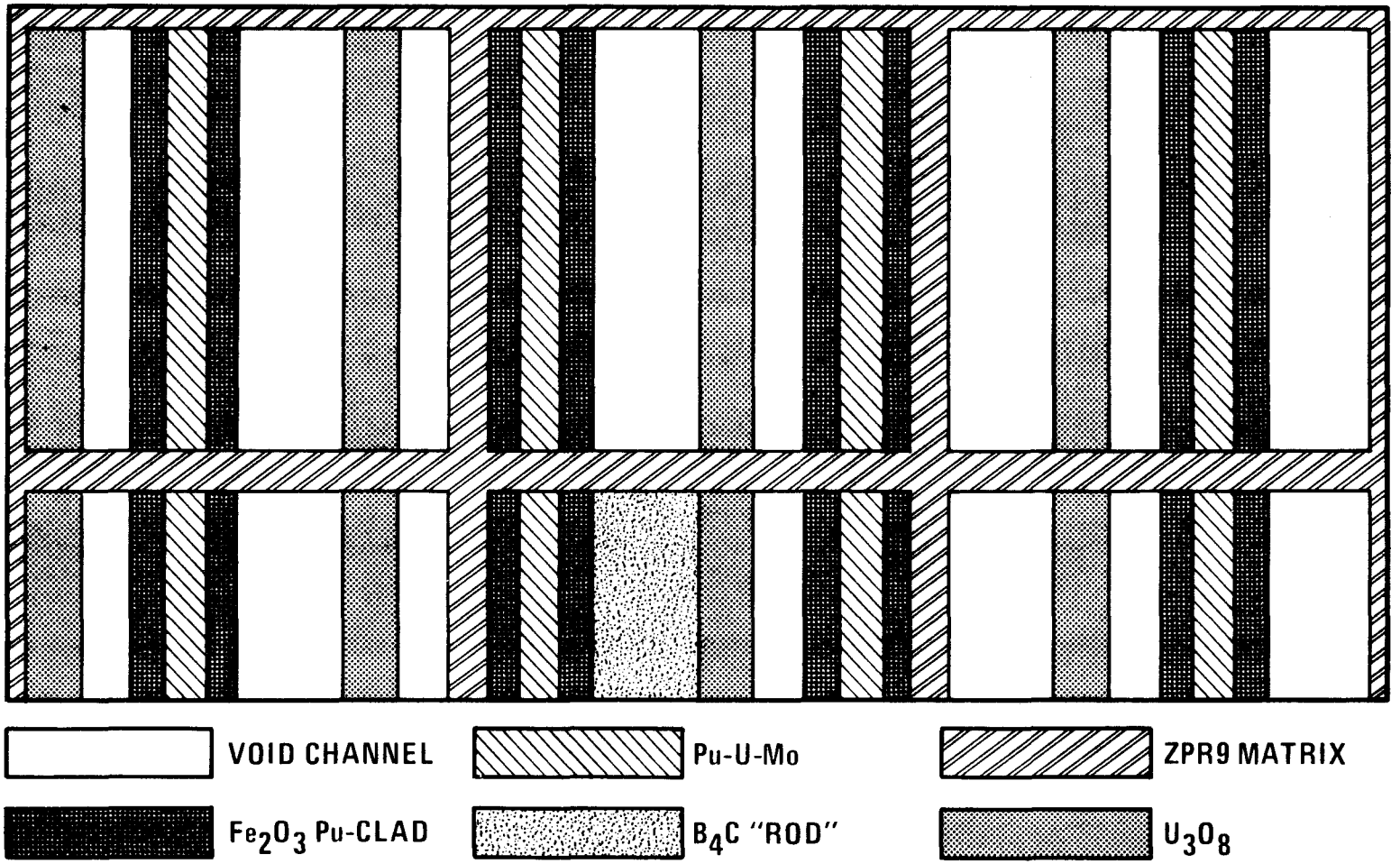

Fig. 2. TWOTRAN model of Phase II core cell with central B_4C column

3. SEQUENCE OF STEAM FLOODING LOADINGS

Table 1 outlines the major steps in the Phase II steam worth program devised by the GA and ANL planners. The sequence shown satisfied the overall objectives of measuring the sensitivity of steam ingress reactivity to variations in reactor configuration and determining the effects of steam in the coolant channels upon basic physics and control parameters of the reactor. Intermediate configurations in addition to those listed were also constructed to satisfy conservative operational procedures required for the ZPR9 critical facility. Approximately 40 different loading changes were involved. The multiple-handling requirements for each assembly drawer during the whole program prompted the use of checkerboard-pattern loadings of flooded and unflooded drawers to simulate intermediate average-channel steam densities. The Appendix of this report includes further details on the fuel loadings, rod patterns, and channel CH_2 floodings for each of the important configurations in the program sequence.

TABLE 1

SEQUENCE OF LOADINGS FOR ANL STEAM-WORTH MEASUREMENTS IN PHASE II GCFR ASSEMBLY

1. Establish reference unrodded configuration (subcritical).
2. Insert CH_2-foam into alternate drawer voids (0.0088 g/cc).
3. Insert CH_2 into remaining core and blanket voids (0.0175 g/cc).
4. Adjust reactivity for physics measurements.
5. Install simulated B_4C control rods; central and center-plus-seven rod ring pattern.
6. Add fuel at core edge to near criticality.
7. Remove CH_2 from channels in two steps (alternate drawers).
8. Reduce core fuel loading.
9. Withdraw B_4C rods in two steps.

4. EXPERIMENTAL RESULTS

Table 2 summarizes the results of the ANL measurements for the worth of simulated steam floodings in the core and blankets for Phase II. Further details on system reactivities for specific configurations and floodings, from which the CH_2 worths were derived, are included in the Appendix.

The first line of data in Table 2 shows that the flooding worth increases nonlinearly as a function of steam density; this property can be ascribed to increased moderation-per-atom of hydrogen because of greater multiple-scattering probability in the channels. The table also shows that increasing the core dimensions reduces the flooding worth for a fixed density, because of a lessened importance of the leakage aspects of the worth. Finally, the table shows that the addition of control poisoning has a significant negative effect on steam worth, as would be expected, because of the reduction of the level and importance of low-energy neutrons.

The configuration listed on the bottom line of Table 2, with the largest core volume and about 6$ worth of control rods installed in a distributed pattern, shows the lowest measured worths of simulated steam flooding. This was a near-critical configuration and the one which was most representative of a real GCFR in a rodded, cold, beginning-of-life loading.

TABLE 2
RESULTS OF ANL EXPERIMENTS FOR WORTHS OF FULL CORE SIMULATED STEAM FLOODING IN PHASE II GCFR ASSEMBLY

Core Configuration		Measured Flooding Worth (Ih)		
Effective Core Radius (cm)[a]	Number of Mockup B_4C Rods Installed	For Nominal Channel CH_2 Density (g/ℓ) of:		
		4.4	8.8	17.5
54.79	None	86.6 ± 10	210.7 ± 14	537.6 ± 10
56.23	None	--	176.5 ± 1.8	484.0 ± 1.8
56.23	Center	--	161.6 ± 5.7[b]	423.6 ± 5.6
56.23	Center + Ring[c]	--	--	357 ± 50
59.38	Center + Ring	--	29.1 ± 2.1	202.0 ± 2.1

[a] Based on loaded fissile mass and cell-average fissile density.

[b] Includes interpolation on reactivity from 56.10 to 56.23 cm configuration.

[c] Pattern of seven rods (Fig. 1) in annulus of average radius 38.90 cm.

5. METHODS USED IN GA ANALYSIS

Figures 3 and 4 chart the course of the analysis carried out for the Phase II steam worths. Further details on the methods and codes utilized at GA have been reported by Merrill (Ref. 7).

5.1. PROCESSING OF ENDF/B-IV BASIC NUCLEAR DATA

Figure 3 shows how basic nuclear data on the ENDF/B tapes are split into three components for a subsequent use in GGC-5 (Ref. 8), the spectrum code in current use at GA for fast reactor analysis. The fine-group average GAM data for structural materials and for fuel isotopes in the range above about 7.5 keV are prepared with GFE4 (Ref. 9). This code has been recently upgraded with an option to average cross-sections using a finite-dilution ($1/\Sigma$-total) flux weighting to effect self-shielding of resonances. For each material processed through GFE4, a dilution factor σ_o is added to the material σ_{total} to provide total scattering-per-material-atom appropriate to the cell mixture involved. Compared to use of a simpler 1/E flux weighting (which yields infinite-dilution cross sections), the new averaging prescription has increased the core and blanket leakage to the extent of a 0.4% reduction in eigenvalue for the basic dry-critical calculations. In addition, the more appropriately shielded scattering data were found to significantly improve steam worth calculations.

The code GAND3 (Ref. 9) processes the resolved-resonance parameters on the ENDF/B tapes to reconstruct, by material, cross section distributions on a hyperfine energy grid (>14,000 points) in the range of 0 to about 7.5 keV. The resulting GAR tape data are used in the GAROL section of GGC-5.

The GANDY (Ref. 10) section of GGC-5 utilizes unresolved-resonance parameters by material derived from the ENDF/B tapes with separate utility codes.

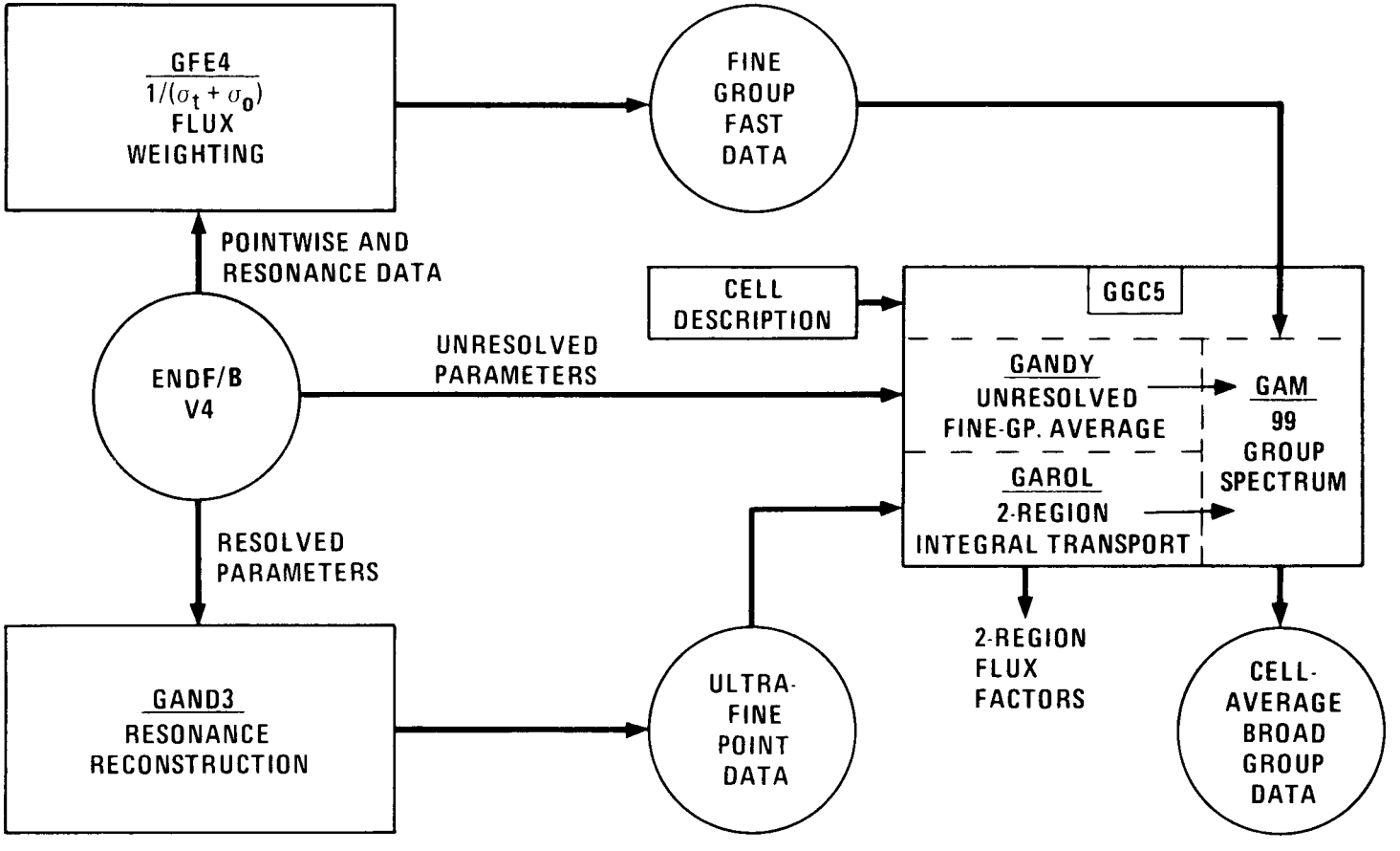

Fig. 3. General Atomic cross section generation for fast reactors

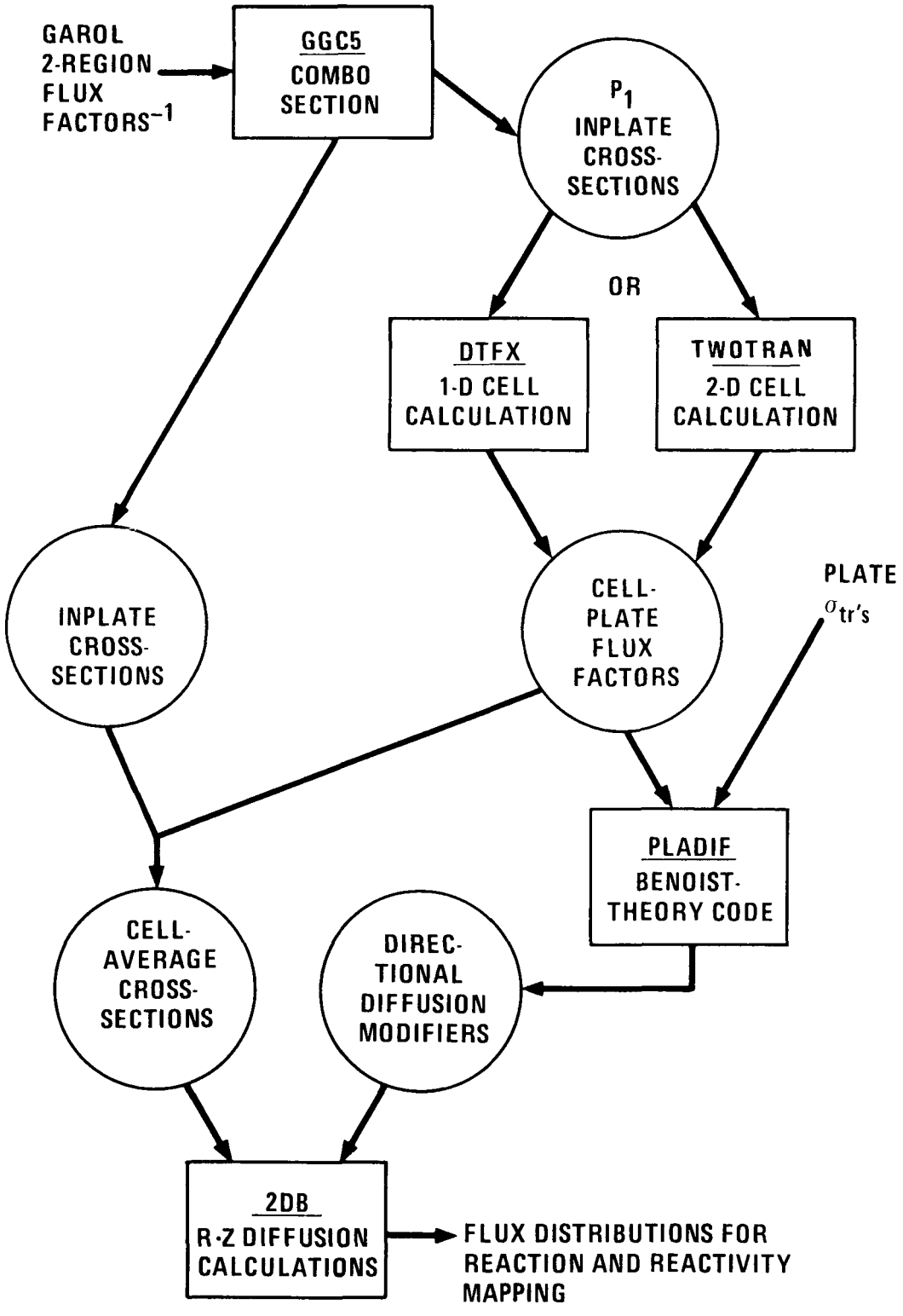

Fig. 4. Adjustments of cross sections for cell heterogeneity

5.2. GENERATION OF BROAD GROUP CROSS SECTIONS

The GAROL section in GGC-5 calculates hyperfine flux distributions in a two-region (fuel/diluent) cell according to integral transport theory and averages cross sections over the fine groups in the resolved range. The method thus accounts for overlapping of resonances for different materials in the fuel region and also for the interactions with structural-material resonances in the diluent region.

The GANDY routine in GGC-5 generates the fine-group cross sections in the unresolved resonance range using the Narrow-Resonance Approximation, accounting for heterogeneity by the equivalence principle with appropriate Dancoff factors.

With all ranges of fine-group data available, the GAM section of GGC-5 carries out a fundamental mode solution of the B_n equations for a homogenized cell composition. The 99-group flux and higher moments thus generated are then used to collapse the fine-group cross sections to the broad-group structures (which in this case are 10- and 28-group sets). Input bucklings, either constant or variable by broad group, are used to represent the spatial distribution effects.

The two-region nature of the GAROL solution requires the running of separate GGC-5 cases for the plates of Pu-U-Mo alloy and U_3O_8 in the core cell. Separate GGC-5 runs were also made for simplified models of the fertile-plate loadings of the radial and axial blanket cells. For the B_4C rod cross sections, another core cell GGC-5 was run with the rod smeared into the diluent region (one column of B_4C in a three-drawer cell).

Thus far, it could be seen that a series of GGC-5 cases is required to generate 10- and 28-group cross sections for the regions of the unperturbed, basic Phase II configuration (the unflooded or "dry" cross section sets). This whole series of GGC-5 runs was then repeated for the core and blanket cells with CH_2 in the void channels, at all three average CH_2 densities, to obtain cross sections appropriately reaveraged in the moderated spectra.

5.3. HETEROGENEITY ADJUSTMENTS

Figure 4 charts the additional procedures involved in adjusting the cross sections to account for the heterogeneous plate structure of the ZPR9 assembly. Inplate cross sections are extracted from the GGC-5 data to set up the regions of the discrete-ordinate core-cell calculations in one and two dimensions. The group ratios of plate-region fluxes to cell-average flux calculated by the transport cases are the heterogeneity (or flux-advantage) factors for correcting the cross sections used in the diffusion theory codes.

As Fig. 2 shows, the TWOTRAN problems modelled the vertical and horizontal cell heterogeneity well and accurately represented the rodded-core-cell case with a B_4C column at the center of nine drawers of core material. Flux factors for a three-drawer central area provided the rod self-shielding effects and also the influence of the B_4C on neighboring fuel and fertile plates. For the unrodded-cell TWOTRAN cases, with and without CH_2 flooding of the void channels, only a 1 x 3 drawer area was modelled. In all TWOTRAN models, the fuel clads were merged with the Fe_2O_3 plates and the cladding of the void channels was homogenized over the channel area to reduce problem complexity. The TWOTRAN studies were carried out only with 10-group cross sections.

For slab-cell calculations, using the one-dimensional discrete-ordinates code DTFX,* all of the distinct regions of the three-drawer core cell through the midplane were modelled explicitly, including true voids (or CH_2), clads for the fuel, voids, and B_4C, etc; the horizontal matrix was smeared in with the vertical steel regions and the void channels. In the DTFX, as well as the TWOTRAN problems, transverse leakage was represented by group pseudo-absorption terms (using cell-average values of axial DB^2) to avoid problems using input bucklings with the low density channels.

Since the B_4C rod mockup extended vertically for only one drawer height,

*DTFX is an extensive GA revision to the one-dimensional transport theory code 1DFX-A (Ref. 11) (D. Mathews, General Atomic Company, private communication).

it would be inappropriate in the DTFX cell calculations to model the rod as an infinite slab at full density. Therefore, the B and C densities were reduced by a factor of 0.805 to produce the same mean optical chord length in the one-dimensional slab as in the two-dimensional model. In essence, this gives the same surface-to-mass ratio for an infinite slab as for the actual B_4C column.

5.4. NEUTRON STREAMING EFFECTS

Conventional diffusion-theory calculations using isotropic diffusion parameters based upon homogenized media are known to substantially underpredict axial neutron leakage through lattices with void or near-void coolant channels, as found in the GCFR or its plate mockup. Benoist (Ref. 12) provided a theory for deriving directional-dependent diffusion coefficients which allows treatment of such anisotropic leakage within the framework of diffusion theory. The code PLADIF, a GA adaptation of an ANL code by Kier (Ref. 13), utilizes the Benoist method to evaluate modifiers to cell-average diffusion coefficients for directions parallel and perpendicular to the plates in a one-dimensional slab-geometry cell. In addition to the inputs indicated in Fig. 4 (the group and region fluxes from DTFX and the material transport cross sections), the PLADIF code uses cell descriptions similar to those used for DTFX. Models of the Phase II cells for PLADIF which were constructed according to methods suggested by Bhattacharyya (Ref. 3), Pond (Ref. 5), and Wade (Ref. 14) are discussed in the Appendix along with some of the PLADIF algorithms.

PLADIF problems were run in both the 10- and 28-group cross section structures for core, radial blanket, and axial blanket cell descriptions. Specific sets of diffusion modifiers were generated for the basic dry configurations (no steam flooding) and for the full-flooding situation, with 17.5 g/ℓ CH_2 in the void slabs. The Appendix includes tabulations of the 28-group modifiers. For intermediate flooding densities at 4.4 and 8.8 g/ℓ of channel CH_2, interpolations between the dry and wet sets were utilized; justification for this approximation for the lower densities is based on Phase I steam-worth studies by Hess (Ref. 4).

Diffusion theory codes at GA have been modified to utilize directional-dependent diffusion coefficients, via input modifiers, to effect the preferential leakage, or streaming, through the coolant channels in either pin geometry or plate geometry. For the calculations in R-Z geometry for Phase II, the PLADIF-output parallel modifiers (D_{11}) were used for the axial (Z) direction, and arithmetic averages of the parallel (D_{11}) and perpendicular (D_1) parameters were used for the radial (R) direction. With this R-Z prescription, the streaming effect for Phase II with reflectors amounts to about -1.7% $\Delta k/k$ in reactivity; i.e., using the modified diffusion parameters lowers the eigenvalue by 1.7% from that calculated using homogeneous diffusion coefficients.

5.5. DIFFUSION THEORY CALCULATIONS

For the Phase II steam worth analysis, a GA modification of the two-dimensional diffusion theory code 2DB (Ref. 15) was utilized. Reactivity changes with configuration were evaluated by eigenvalue difference. Exact perturbation methods were found unnecessary because of the fast and accurate convergence obtainable with the 2DB code. Adjoint flux calculations using 2DB gave eigenvalues that were identical within the convergence specifications to the corresponding eigenvalues from the forward flux solutions. Effective delayed neutron parameters (for reactivity conversion) and central worths of small samples were then calculated using the perturbation-theory code PERT (Ref. 16), which also uses directional diffusion coefficients.

In the 2DB problems, the Phase II configuration of Fig. 1 was modelled in R-Z geometry, incuding core, blanket, and reflector regions, both axially and radially. Also, extra steel material was added about the assembly periphery to account for the effects of the ZPR9 structural components (matrix, knees, etc.) beyond the reflectors. The central control rod mockup was modelled with a homogenization of rod and core material in a three-drawer area. The ring of seven rods was smeared into an annular ring having the area of 42 matrix drawers at the average rod radius.

6. STUDIES OF HETEROGENEITY MODELLING

Since the reactivity worth of steam entry is the net result of a relatively small difference between large negative and positive reactivity worth components, calculated steam worths are found to be highly sensitive to analytical approximations. As part of the investigations of steam worth sensitivity to methodologies, an extensive study was carried out with different models of the Phase II core-cell heterogeneity. In addition to examination of the differences in one- and two-dimensional transport treatments, the effects of various other options were studied, including (1) plate mesh spacings, (2) scattering order, (3) quadrature, and (4) the prescription used in slab geometry for representing the fuel columns, with an accounting for the vertical discontinuities imposed by the horizontal matrix structure. The two following basic problems became apparent:

1. The uncertainties in the basic cell plate heterogeneity factors and the resulting uncertainties in configuration eigenvalues and clean-core steam worths.

2. The method-dependent differences in self-shielding factors for the B_4C rod mockup and the resulting uncertainties in calculated rod worths and calculations of rodded-core steam worths.

6.1. FUEL PLATE HETEROGENEITY FACTORS

Table 3 compares the fuel-plate (Pu-U-Mo) flux advantage factors given by the one- and two-dimensional discrete-ordinate transport calculations, both with and without simulated steam flooding. The TWOTRAN treatment gives slightly higher factors than the DTFX, especially in the highest and lowest energy groups. In terms of reactivity, these flux-advantage factor differences produce eigenvalue differences of $+7.5 \times 10^{-4}$ and 5.5×10^{-4} for the

TABLE 3
EFFECTS OF HETEROGENEITY MODELLING ON CALCULATED EIGENVALUES AND STEAM WORTHS

Cell Calculation	DTFX-P_1		TWOTRAN-P_1	
Mesh Intervals Quadrature	92 S_{16}-Double Pn		10x50 S_8-Double Pn-Tn	
Void channel CH_2 density, (g/ℓ^2)	None	17.5	None	17.5
Flux factors for Pu-U-Mo plate:				
Group 1	1.163	1.167	1.173	1.178
2	1.085	1.090	1.083	1.093
3	1.027	1.033	1.028	1.034
4	1.010	1.016	1.011	1.016
5	0.997	1.001	0.997	1.008
6	0.993	0.991	0.994	0.992
7	0.984	0.982	0.984	0.982
8	0.971	0.960	0.974	0.964
9	0.948	0.932	0.949	0.934
10	0.876	0.825	0.884	0.830
Configuration:				
Loading	136	112	136	112
Core radius	56.23 cm	56.23 cm	56.23 cm	56.23 cm
B_4C rods	None	None	None	None
2DB eigenvalue	0.98762	0.99384	0.98836	0.99438
17.5 g/ℓ flooding worth	598 Ih		577 Ih	

dry and wet cases, respectively. The net effect on clean-core steam worths is then about 2×10^{-4}, or a +20 inhour (Ih) difference between the 1-D and 2-D cell treatments.

For the DTFX problems cited in Table 3, the fuel plates were modelled with four mesh intervals, and a density factor of 0.948 was used to produce a surface-to-mass ratio equivalent to the effective ratio in the fuel stack, with an adjustment for plate-to-plate transmission probability. A simple smearing of the fuel columns over the matrix-unit height would give a density factor of about 0.91. Variations of the density factor used for Pu in the DTFX cases gave changes on the order of the DTFX/TWOTRAN differences seen in Table 3. However, agreement with the group-1 factor (to the 1.17 TWOTRAN value) required a density factor of 1.0, which considerably worsened the lowest-group agreements by increasing the absorption self-shielding.

Varying the mesh structure in the DTFX cases between three and six intervals for the Pu-U-Mo had no effect on high-energy factors but slightly reduced the factors in groups 7 through 10. The use of P_3 anisotropic scattering cross-sections was found completely unnecessary for the dry cases but was not investigated for the CH_2-flooded cases. Changes in quadrature had only minor effects on factors in groups 1 through 3 and little or no influence on the low-energy group factors, from order S_{12} up; however, it is essential to use the double-P_n quadrature scheme for slab geometry. Correspondingly, for the best TWOTRAN cases an S_8 angular order was specified, utilizing a double-P_n quadrature for the direction perpendicular to the plates and different-order Tschebyschev quadratures (by DP_n level) for the directions parallel to the plate columns.

Overall, considering the variances in cell-plate flux factors observed from use of different models and assumptions, there appears a basic uncertainty of about 6×10^{-4} in calculated eigenvalues from possible errors in heterogeneity adjustments. For analyses carried out with consistent models, the uncertainty for the reactivity changes with configuration, as for steam worth, is probably on the order of 4×10^{-4}, or ±40 Ih.

6.2. SELF-SHIELDING OF B_4C ROD MOCKUP

The modelling of the isolated B_4C rod mockups in one-dimensional geometry posed a more severe problem. Table 4 compares the DTFX and TWOTRAN generated flux factors for the 1.27 x 5.08-cm B_4C column in the dry and wet Phase II core cells. In the DTFX model, six mesh intervals were used across the B_4C width compared with a 4 x 9 mesh in the TWOTRAN model. A B_4C density factor of 0.804 was used in DTFX to give the same mass-to-surface ratio as for the full-density plate in TWOTRAN.

For the dry rodded cell, a comparison of data columns 1 and 2 in Table 4 shows generally fair agreement of DTFX and TWOTRAN results, with slightly higher high-energy factors and slightly lower low-energy factors given by DTFX. Overall, for the dry configurations, the rod worths calculated using the DTFX and TWOTRAN factors agree to within 0.5%.

For the wet rodded cell, the last two columns in Table 4 indicate more self-shielding for the low groups by DTFX than by TWOTRAN calculations. Here the modelling differences translate into rod worth differences of 2 to 3%, a relatively small uncertainty. However, for the fully rodded situation (~2000 Ih of installed poison), the 3% difference translates into a ±60 Ih uncertainty, which would carry over into the evaluation of rodded-core steam worth.

No variations of the rodded-cell DTFX specifications were able to reduce rod flux factors of groups 1 through 4 to the TWOTRAN values, presumably because of the problem in modelling the fuel-plate proximity (see Fig. 2). The low energy factors (groups 7 through 10) in the slab-cell cases were insensitive to changes in quadrature but were affected by density and mesh assignments. Using the full plate density for the B_4C slab in DTFX would have increased self-shielding and worsened the agreement with TWOTRAN. Thus, for both poison and fuel plate types, the use of effective mass-to-surface ratios as density factors in the one-dimensional slabs largely provides for correct self-shielding of absorptions in the low energy range.

TABLE 4
COMPARISON OF METHODS FOR CALCULATING ROD SELF-SHIELDING FACTORS
USING 10-GROUP CROSS SECTIONS

Configuration	Dry, Core Radius = 56.2 cm		56.2 cm Core with 17.5 g/ℓ Channel CH_2	
Cell Calculation	DTFX	TWOTRAN	DTFX	TWOTRAN
Mesh Intervals	92	30x50	92	30x50
Quadrature	$S_{12}DP_n$	$S_8DP_nT_n$	$S_{12}DP_n$	$S_8DP_nT_n$
Shielding factors for B_4C:				
Group 1	0.939	0.919	0.938	0.918
2	0.946	0.936	0.947	0.936
3	0.921	0.915	0.928	0.921
4	0.955	0.953	0.965	0.961
5	0.950	0.948	0.962	0.961
6	1.007	1.006	1.003	1.004
7	0.920	0.916	0.904	0.905
8	0.920	0.935	0.842	0.869
9	0.793	0.801	0.672	0.713
10	0.570	0.556	0.328	0.390
Calculated rod worth (Ih)				
Center rod	-474.0	-475.6	-514.0	-525.8
Center + seven-rod ring	-1912	-1922	-2075	-2138

Another aspect of DTFX and TWOTRAN input specifications which can be varied is the representative spatial leakage effect (via DB^2 pseudo absorption cross sections). For the rodded-cell cases in Table 4, axial bucklings for a 3 x 3 drawer region (with rod at the center) were used to provide transverse leakage by group. Selection of other buckling sets, such as those for larger regions or for full radial-plus-axial leakage, can produce variations of shielding factors similar to the DTFX/TWOTRAN differences shown in Table 4.

7. WORTHS OF MOCKUP B_4C CONTROL RODS

As the first stage in reviewing the analysis of the CH_2-flooding effects, it is worthwhile to examine the results of rod worth calculations with and without the CH_2 ingress. Table 5 summarizes the details and results of the Phase II rod worth measurements and gives comparisons with worths calculated by various methods via calculated-to-experimental (C/E) ratios.

7.1. TOTAL SHIELDING VERSUS CH_2 FLOODING DENSITY

Table 5 includes a column of 10-group results for rod worths calculated using normal-core-cell DTFX flux factors for fuel materials but without shielding factors for the B_4C cross sections. For the dry configurations, disregarding the rod shielding produces rod worths up to 10% greater than the calculations with factors, indicating a 1-group average shield factor of about 0.90 in the normal core for this plate-column rod. For the flooded environments, however, the shielding effects increase dramatically, and errors in calculated rod worths of up to +50% would be incurred by disregarding the rod internal shielding. In terms of the absolute reactivity for one rod, the error would be on the same order as the total worth for the steam at the densities studied.

7.2. 10-GROUP ROD WORTH ANALYSES

The C/E values in columns 7 and 8 of Table 5 are for the 10-group calculations of rod worths quoted in Table 4 using DTFX- and TWOTRAN-derived shielding factors. For the dry configurations, both shielding-factor sets give fairly good agreement with measured single and 8-rod worths. In the case having 17.5 g/ℓ channel CH_2, the single rod worths calculated using DTFX and TWOTRAN factors are both lower than measurements, by 5.6 and

TABLE 5
COMPARISONS OF MEASURED AND CALCULATED WORTHS OF MOCKUP B_4C RODS IN PHASE II GCFR ASSEMBLY WITH AND WITHOUT SIMULATED STEAM FLOODING

Assembly Configuration		B_4C Rods Installed[a]		Measured Total Worth of Rods (Ih)	Calculated-to-Experimental Ratios			
					10-Group Analysis			28-Group Analysis Using DTFX Factors
Void Channel CH_2 (g/ℓ)	Core Radius (cm)	No.	Loading Change		No B_4C Shielding	DTFX Shielding Factors	TWOTRAN Shielding Factors	
Dry	56.23	1	136/135	-484.2 ± 4.6	1.05	0.978	0.982	0.980
Dry	56.23	8	136/134	-1934 ± 34	1.08	0.989	0.994	0.999
8.8	56.10	1	81/82	-499.1 ± 4.1	1.19	0.998	--	0.992
17.5	56.23	1	112/113	-544.6 ± 3.7	1.46	0.944	0.966	0.936
17.5	56.23	8	112/114	-2061 ± 33	1.31	1.007	1.037	1.005

[a] Single rod at core center; eight-rod pattern is center rod plus seven rods in a ring having average radius of 38.9 cm.

3.4%, respectively. Possible explanations for this underprediction of flooded rod worth include (1) B_4C-plate flux factors which are too low because of excessive moderation by the CH_2 in the cell calculations, (2) too hard a spectrum given by the 2DB runs with CH_2, (3) B-10 cross sections in ENDF/B which are too low at lower energies, and (4) an approximate accounting for the effect of the B_4C plate on the resonance-shielding of U-238 cross sections for the U_3O_8 plates in the rodded three-drawer cell.

7.3. 28-GROUP ROD WORTH ANALYSIS

A comparison of the seventh and last columns of Table 5 shows excellent agreement, to within 1%, between 28- and 10-group analyses of B_4C rod worths, with and without simulated steam flooding. For both analyses, consistent treatments with the same one-dimensional DTFX cell model were used to derive heterogeneity and shielding factors in the respective group structures.

7.4. SINGLE VERSUS 8-ROD WORTHS

For the unflooded situation, the measured worth of the eight-rod combination was a factor of 3.99 times the central-rod worth. Calculations for the dry cases gave corresponding ratios in good agreement with experiments; i.e., values of 4.04, 4.04, and 4.07 using 10-group TWOTRAN, 10-group DTFX, and 28-group DTFX shielding factors, respectively, were obtained. With full steam flooding (17.5 g/ℓ), the calculated 8-rod/1-rod worth ratios were virtually identical to the dry cases: 4.06, 4.04, and 4.06. However, the measurements in the wet cases show a worth ratio of only 3.78 ± 0.06. The discrepancy is evident in the last two lines of calculated results in Table 5, where C/Es increase from 0.94 for center-rod worths to 1.01 for 8-rod worths.

The discrepancy noted is probably a result of the known deficiency in the modelling of the seven outer-rod pattern as an annular ring in the 2DB calculations. Although the asymmetry may have been unimportant in the dry reactor, flux tilting by the pattern in the flooded case was probably

more severe, especially with the highly moderated flux spectrum. Calculations with XY-geometry will be required to resolve this question.

7.5. ENHANCEMENT OF ROD WORTHS BY STEAM

It is appropriate to examine here the implications of the experimental data about rod designs. The simulated steam ingress has been shown to progressively enhance the worths of the mockup control rods. At the maximum flooding density, the rod effects are 12% higher than in the dry case. However, the small-sample worth of B-10 at the center of the wet core was about 45% greater than the corresponding worth measured in the dry core. The fact that the wet-to-dry worth ratio for the mockup rod is so much less than the wet-to-dry ratio for the small-sample worth is a result of the extensive self-shielding in the 1.27-cm-thick plate of B_4C used as the rod. Thus, further enhancement of the rod worth could have been achieved with a mockup design utilizing rods or plates of smaller mean chord length. Future critical experiments for the GCFR should include studies on steam enhancement potentials of various rod designs and materials.

The calculated enhancement effects from flooding are less than those measured, ranging (for the central rod) from +7.5 for the dry case to +10.5% for the 17.5 g/cc CH_2 case in the voids. (See Section 7.2 for possible reasons for the discrepancies.)

8. STEAM WORTH SENSITIVITY TO ANALYTICAL APPROXIMATIONS

8.1. EFFECTS OF METHODS ON CLEAN-CORE CH_2 WORTH

Table 6 shows how changes in methods for treating resonance and cell-spatial shielding affect the calculations of the worth of simulated steam flooding in unrodded Phase II configurations. The improvement in the 10-group results shown in data rows 1 and 2 of the table, from a C/E of 2.08 to 1.30, is a result of the improved shielding of scattering resonances in GFE4. Another 5% reduction in calculated worth, at 17.5 g/ℓ flooding, was obtained from a more rigorous DTFX evaluation of cell-plate factors for broad-group cross sections in the resolved range than is provided by the two-region GAROL treatment in GGC-5 (row 4 versus row 2 data in Table 6). Also, the TWOTRAN evaluation for flux factors in the clean cell gives a 4% lower flooding worth than is calculated using the DTFX factors.

For the 28-group cases, the change from a 1/E to a $1/\Sigma_t$ flux for averaging of the fine group cross sections and the utilization of DTFX heterogeneity factors over all groups combine to reduce the C/E from 2.30 to 1.00 for the calculated worth of the full density (17.5 g/ℓ CH_2) steam flooding. At the lower density floodings, 4.4 and 8.8 g/ℓ average channel CH_2, the effect of another approximation was investigated. For the experiments, these lower density floodings were simulated using full density perforated CH_2 foam inserted into voids of only one quarter or one half of the drawers. Lumping of the CH_2 in the void channels of the DTFX cell calculations, in rough correspondence with experiment, is found to appreciably affect the resulting steam worth calculations. Compared with smearing the CH_2 into all cell void channels, the lumped case factors produce higher steam worths, by about 32 and 18 Ih, respectively, for the 4.4 and 8.8 g/ℓ average CH_2 densities. Thus, the more approximate the smearing assumption, the larger the likely error of the calculated flooding worth.

TABLE 6
EFFECTS OF METHOD VARIATIONS ON CALCULATIONS OF CLEAN CORE STEAM WORTHS

Methods and Analytical Options					Calculated-to-Experimental Ratios (C/E) for Flooding of:		
No. of Broad Groups	GFE4 Flux Weighting for Fine-Group σ_s	Broad Group Heterogeneity Factors: High Energy Range	Broad Group Heterogeneity Factors: Resolved Resonance Range	Distribution of CH_2 in Cell-Model Channels	4.4 g/ℓ CH_2 in Voids: 54.8-cm core (E = 86 ± 10 Ih)	8.8 g/ℓ CH_2 in Voids: 56.2-cm core (E = 177 ± 2 Ih)	17.5 g/ℓ CH_2 in Voids: 56.2-cm core (E = 484 ± 2 Ih)
10	1/E	DTFX	GAROL	Smeared	--	--	2.08
10	$1/\Sigma_{tot}$	DTFX	GAROL	Smeared	1.31	1.53	1.30
10	$1/\Sigma_{tot}$	TWOTRAN	TWOTRAN	Smeared	--	--	1.19
10	$1/\Sigma_{tot}$	DTFX	DTFX	Smeared	--	1.52	1.24
28	1/E	DTFX	GAROL	Smeared	--	--	2.32
28	$1/\Sigma_{tot}$	DTFX	DTFX	Smeared	0.50	0.84	1.00
28	$1/\Sigma_{tot}$	DTFX	DTFX	Lumped[a]	0.87	0.94	1.00

[a] For intermediate densities (4.4 and 8.8 g/ℓ average in channels), full 17.5 g/ℓ CH_2 assigned to 1/4 or 1/2 of cell-model void channels, similar to experimental procedure.

8.2. EFFECTS OF METHODS ON RODDED CORE CH_2 WORTHS

The effects of heterogeneity treatments on the steam worth calculations for configurations with eight B_4C rods installed are shown in Table 7; included are two 10-group cases and one 28-group case where no shielding at all was provided for the boron cross sections (factors of 1.0) for the rod regions. For the first 10-group case in Table 7, the error from neglecting rod shielding nearly compensates for the error caused by the 1/E fine-group flux weighting. Line two of the data indicates that omitting the B_4C rod shielding alone gives negative or low steam worths, in considerable error from measurements. The TWOTRAN treatment for B_4C shielding and other cell factors gives a 20% lower rodded core steam worth than the DTFX treatment, because of the 3% effect on the flooded core rod worths mentioned in Section 6.

In the last line of Table 7 are found the best overall agreements with measurements, when the most rigorous calculational methods are employed; these methods include $1/\Sigma_t$ GFE4 flux weighting, 28-group cross sections, lumped CH_2 in cell channels, full range cell flux factors, and appropriate rod shielding. Future improvements of both basic data and methods will undoubtedly alter the results of steam worth calculations, but the effects are not expected to be as severe as those resulting from the more gross approximations in the Tables 6 and 7 cases.

TABLE 7
EFFECTS OF METHOD VARIATIONS ON CALCULATIONS OF STEAM WORTH IN RODDED-CORE PHASE II CONFIGURATIONS

Methods and Analytical Options						Calculated-to-Experiment Ratio (C/E) for Flooding of:		
No. of Broad Groups	GFE4 Flux Weighting for Fine-Group σ_s	Broad-Group Heterogeneity Factors: High Energy Range	Broad-Group Heterogeneity Factors: Resolved Resonance Range	Broad-Group Heterogeneity Factors: B_4C Rod Shielding	Distribution[a] of CH_2 in Cell-Model Channels	8.8 g/ℓ: 59.4-cm Core with 8 B_4C Rods (E = 29 ± 2 Ih)	17.5 g/ℓ: 59.4-cm Core with 8 B_4C Rods (E = 202 ± 2 Ih)	17.5 g/ℓ: 56.2-cm Core with 8 B_4C Rods (E = 357 ± 50 Ih)
10	1/E	DTFX	GAROL	None	Smear	--	1.21	1.10
10	$1/\Sigma_{tot}$	DTFX	GAROL	None	Smear	-2.86	-0.46	0.07
10	$1/\Sigma_{tot}$	TWOTRAN	TWOTRAN	TWOTRAN	Smear	--	--	1.01
10	$1/\Sigma_{tot}$	DTFX	DTFX	DTFX	Smear	3.56	1.48	1.22
28	1/E	DTFX	GAROL	None	Smear	--	1.86	1.51
28	$1/\Sigma_{tot}$	DTFX	DTFX	DTFX	Smear	-0.27	1.04	0.97
28	$1/\Sigma_{tot}$	DTFX	DTFX	DTFX	Lumped	0.85	1.04	0.97

[a] Referring to representation for 8.8 g/ℓ CH_2 channel average: Experiment utilized CH_2 foam at 17.5 g/ℓ in alternate-drawer voids, or a "lumped" distribution.

9. COMPARISONS OF MEASURED AND CALCULATED FLOODING WORTHS

9.1. FINAL 10-GROUP ANALYSIS

Table 8 lists the results of the clean and rodded core steam worth calculations using 10-group cross sections with heterogeneity factors derived from one-dimensional cell calculations. The last C/E for the 8.8 g/ℓ cases looks poor on first glance, but in terms of difference from the experiments rather than ratio, the result is closer (+75 Ih) than in the higher rows (C-E = +83 to 99 Ih). At the 17.5 g/ℓ flooding density, the C/Es appear similar to the factors for the central worth discrepancies for light-elements. For safety analyses, consequently, 10-group analyses would be only marginally adequate for evaluating steam reactivity worth, and only then if it can be shown that 10-group evaluations consistently overpredict steam worth as a result of identified approximations.

9.2. FINAL 28-GROUP ANALYSIS

Table 9 shows the clean and rodded flooding worths for Phase II calculated using 28-group cross sections, again with DTFX-generated shielding factors for the plates of fuel, U_3O_8, B_4C, etc. Like the measurements and the 10-group results, the 28-group flooding worth measurements decrease with increasing core dimensions and with additions of control poisoning. The agreement of these 28-group calculations with experiments is quite satisfactory, indeed perhaps surprising in view of the steam worth sensitivity to a great many analytical facets.

Comparisons of C/E values for rodded versus unrodded flooding cases in Table 9 as well as in Table 8 demonstrate that the rodded core steam worths can be predicted with the same accuracy as steam worths in an

TABLE 8
SUMMARY OF FINAL 10-GROUP ANALYSIS FOR WORTHS OF
SIMULATED STEAM FLOODING IN PHASE II GCFR ASSEMBLY

Configuration		Steam Flooding (g/ℓ CH_2 in Void Channels)	10-Group Calculations Using DTFX Heterogeneity Factors		
Core Radius (cm)	No. of B_4C Rods Installed		Calculated Flooding Worth (Ih)	C/E	C-E (Ih)[a]
54.79	None	8.8	309	1.47	98 ± 14
54.79	None	17.5	671	1.25	134 ± 10
56.23	None	8.8	269	1.52	92 ± 2
56.23	None	17.5	598	1.24	114 ± 2
56.23	1	8.8	247	1.53	85 ± 6
56.23	1	17.5	557	1.32	134 ± 6
56.23	8	17.5	434	1.22	77 ± 50
59.38	8	8.8	104	3.56	75 ± 2
59.38	8	17.5	298	1.48	96 ± 2

[a] Uncertainty assigned for measurements only.

TABLE 9
SUMMARY OF FINAL 28-GROUP ANALYSIS FOR WORTHS OF
SIMULATED STEAM FLOODING IN PHASE II GCFR ASSEMBLY

Configuration		Steam Flooding (g/ℓ CH_2 in Void Channels)	28-Group Calculations Using DTFX Heterogeneity Factors		
Core Radius (cm)	No. of B_4C Rods Installed[a]		Calculated Flooding Worth (Ih)	C/E	C-E (Ih)[a]
54.79	None	4.4	75	0.86	-12 ± 10
54.79	None	8.8	203	0.96	-8 ± 14
54.79	None	17.5	555	1.03	+18 ± 10
56.23	None	8.8	165	0.94	-12 ± 2
56.23	None	17.5	484	1.00	0 ± 2
56.23	1	8.8	145	0.90	-16 ± 6
56.23	1	17.5	449	1.06	+25 ± 6
56.23	8	17.5	345	0.97	-12 ± 50
59.38	8	8.8	24.6	0.84	-5 ± 2
59.38	8	17.5	209	1.04	+7 ± 2

[a] Uncertainty assigned for measurements only.

unpoisoned reactor, with the proviso that a reasonable effort be expended in re-evaluation of self-shielding effects for control rods in each of the different steam environments.

9.3. CALCULATED/EXPERIMENTAL DIFFERENTIAL

In addition to the C/Es for flooding worths, both Tables 8 and 9 include evaluations of the analyses via differences between calculated and experimental results (C-E values). As with the sodium-voiding reactivity effect in an LMFBR, steam worth is a balance of competing positive and negative components, and thus examination of the C-E differential is more relevant.

In the 10-group results of Table 8, there appears a positive calculational worth bias of about 100 Ih, overall, with a standard deviation of ± 22 Ih. For comparable configurations at the two different densities the biases are somewhat different, +88 ± 11 Ih for 8.8 g/ℓ channel CH_2 and +120 ± 24 Ih for 17.5 g/ℓ channel CH_2; the lower values for the 8.8 g/ℓ cases may reflect the approximation of smearing the CH_2 into all void channels in the cell model used in the 10-group DTFX problems for that density.

In Table 9, for the 28-group results the average C-E differential for steam worth in the ten configurations is -2 Ih with a standard deviation of ± 14 Ih. The spread of the differential is about 40 Ih, which is within the estimated ± 60 Ih uncertainty that could be assigned to the analysis through evaluations of cell-heterogeneity corrections to cross sections. The 8.8 g/ℓ and 17.5 g/ℓ C-E bias sets are closer for 28 groups, giving -10 ± 5 Ih and +8 ± 15 Ih, respectively.

Thus there has been observed a relatively constant bias of about +100 Ih for the 10-group steam worth calculations as compared to the 28-group results, with only a slight variation with rod poisoning (+110 Ih bias for clean configurations versus +89 Ih for rodded cases). Also, for steam flooding of 8.8 and 17.5 g/ℓ, the 10/28 bias varies only slightly, about 10 Ih. This discrepancy for the coarser energy-mesh approximation

can be attributed to several analytical stages, ranging from the 2DB cases through the collapsing of cross sections by GGC-5. Basic configuration eigenvalues given by 10- and 28-group 2DBs agree much more closely for the flooded loadings than for the dry cases. This suggests that the 99-group spectra generated by GGC-5 for subsequent collapsing of both 10- and 28-group cross section sets are better calculated with the cell CH_2 additions than are those for the dry case.

9.4. GRAPHIC COMPARISONS

Figure 5 plots the measured and calculated flooding worths versus density with the smallest clean core configuration. The 10-group analysis is seen to consistently overpredict the CH_2 worths. The 28-group curve initially undershoots the experimental values and then slightly exceeds them at the highest density, but has overall agreement to ± 25 Ih.

Plotted in Fig. 6 are the steam worth results for the largest Phase II core configuration with 6$ worth of installed control poisoning. Again, the overprediction by the 10-group analysis is seen, but with approximately the same 100 Ih spread as for the clean-core case.

The 28-group results plotted in Fig. 6 for rodded Phase II steam worth coincide with the measurements to within ± 10 Ih. With an initial negative slope and an upwards curvature, this curve for the most representative GCFR situation, although having an estimated shape based upon only two calculational points, is typical of the curves generated for steam worth versus density in past GCFR demonstration plant safety analyses. For the cold mockup Phase II configuration, however, the curve crosses to positive at a relatively low density (0.5% steam).

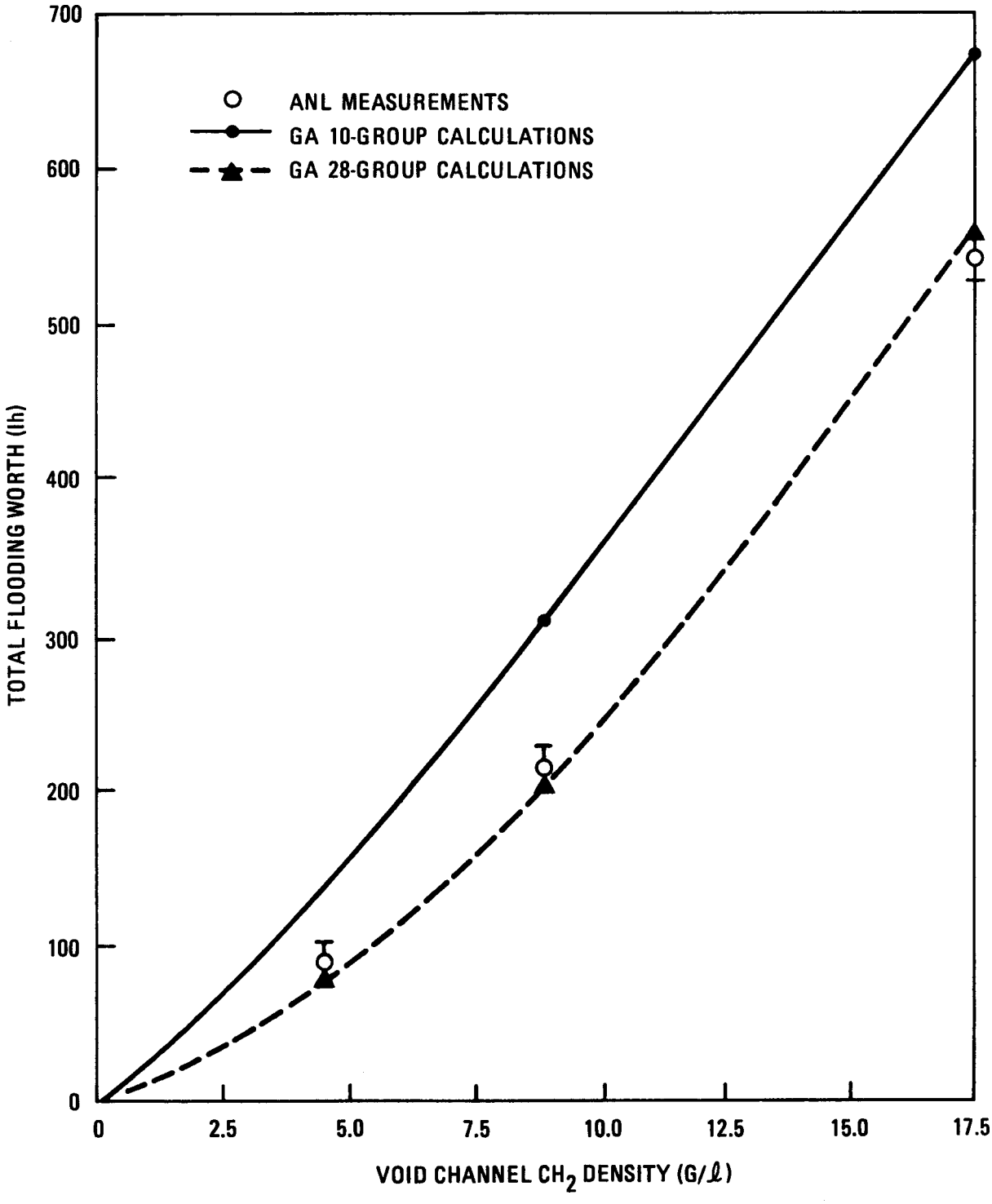

Fig. 5. Worth of simulated steam flooding in unrodded Phase II GCFR assembly with 1150-ℓ core

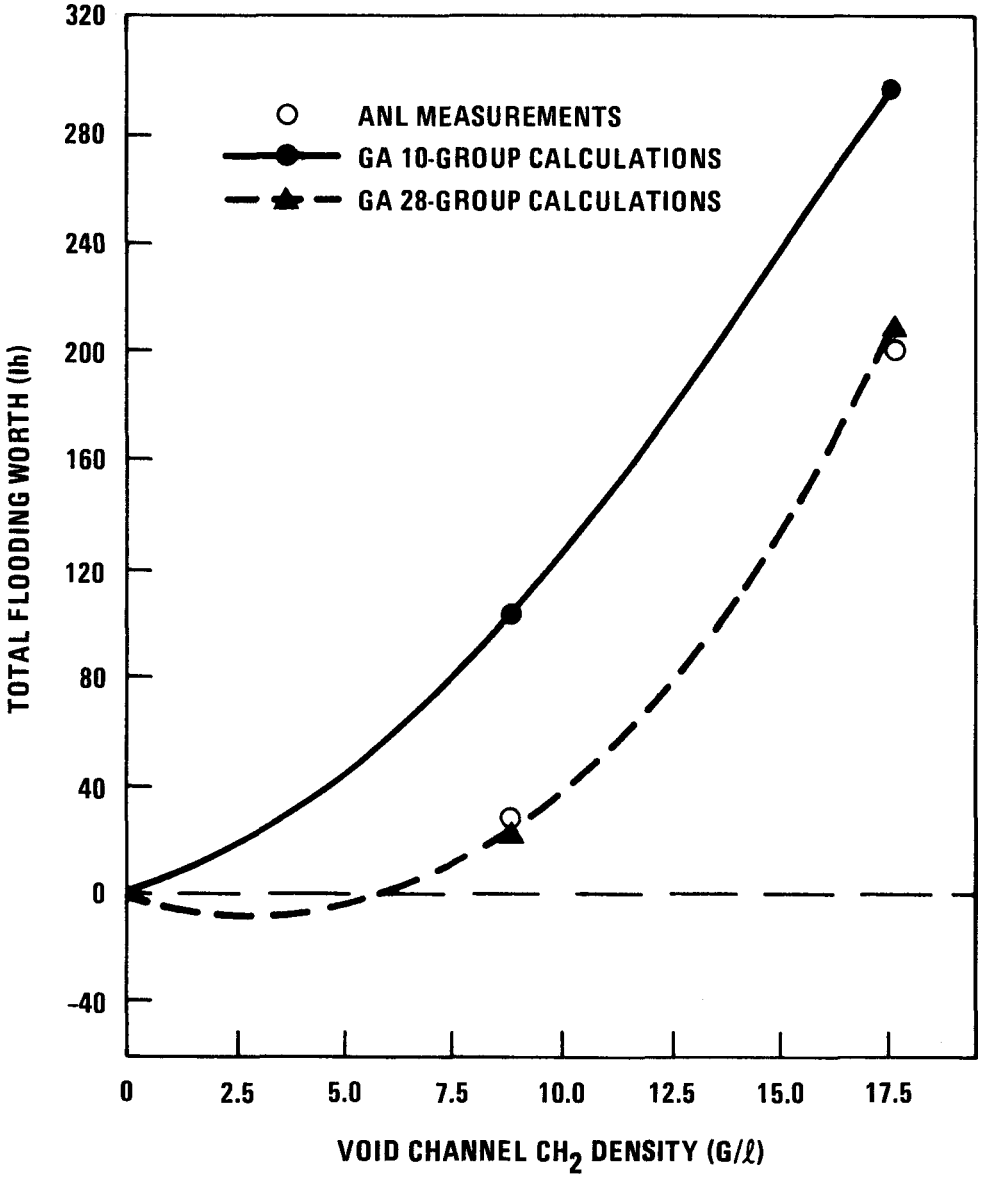

Fig. 6. Worth of simulated steam flooding in Phase II GCFR assembly with eight B_4C rods in a 1350-ℓ core

10. EFFECTS OF STEAM INGRESS ON REACTIVITY COEFFICIENTS

The worths of small samples of various core materials were measured at the center of the Phase II core in both the normal and the full density steam-flooded condition (17.5 g/ℓ CH_2 in all void channels). These experiments were part of the program for defining the influence of simulated steam flooding on basic physics characteristics. Table 10 compares the Phase II measured material worths with coefficients calculated using 28-group perturbation theory; included are the ratios of worths in the wet core to those in the unflooded core given by measurements and by calculations.

For the fuel isotopes, the basic C/Es, with and without steam flooding, are typical of the central worth discrepancies noted in LMFBR or other fast reactor analysis, i.e., C/Es in the range of 1.10 to 1.30. The calculated worths of carbon appear anomalously high, especially in the flooded case. While the B-10 coefficient is well predicted for the dry core, an overprediction by 14% is given by the wet core calculation; this may suggest that the wet case analysis gives an over-moderated spectrum. However, since the C/E for B-10 is closer to the fuel worth C/Es in the wet core than in the dry core, it is possible the steam case spectrum is better calculated and the general central worth discrepancy is caused by other data or analytical errors.

The experiments show significant impact of the steam ingress on material reactivity coefficients, particularly for samples of hydrogenous material, B-10 and carbon, with lesser but important effects for U-238, Pu-240, and Pu-241. Worths for the Pu-239 and U-235, however, are little affected by steam. The calculations predict fairly well the measured impacts except for the CH_2 samples, where it is recognized that the first order perturbation theory is completely inappropriate. The calculations also reveal an

TABLE 10
COMPARISONS OF MEASURED AND CALCULATED CENTRAL REACTIVITY COEFFICIENTS IN PHASE II GCFR ASSEMBLY WITH AND WITHOUT SIMULATED STEAM INGRESS

Sample Material	Center of Dry Core		Center of Wet Core (17.5 g/ℓ Channel CH_2)		Wet/Dry Worth Ratios		
	Measured Worths (Ih/kg)	28-Group Analysis, C/E[a]	Measured Worths (Ih/kg)	28-Group Analysis, C/E[a]	Experiments	28-Group Analysis	10-Group Analysis
CH_2	159 ± 7	-0.26	329 + 11	0.93	2.06	7.41	-0.67
B-10	-3412 ± 51	1.03	-4934 + 66	1.14	1.45	1.60	1.57
C	-21.6 ± 0.8	1.62	-7.9 + 0.4	2.29	0.37	0.52	0.48
Steel	-7.6 ± 0.1	1.20	-7.4 + 0.1	1.24	0.97	1.00	0.93
Mn	-10.6 ± 0.6	1.42	--	--	--	1.69	1.77
U-235	170 ± 2	1.18	177 + 2	1.21	1.04	1.07	1.03
U-238	-11.3 ± 0.3	1.06	-13.3 + 0.4	1.05	1.18	1.18	1.14
Pu-239	238 ± 2	1.16	238 + 2	1.18	1.00	1.02	0.98
Pu-240	42.8 ± 0.5	1.27	34.6 + 0.3	1.15	0.81	0.73	0.71
Pu-241	292 ± 3	1.25	338 + 2	1.17	1.16	1.08	1.08

[a] Calculated-to-experimental ratio (C/E) for worths derived using first-order perturbation theory.

appreciable change for the worth of Mn, a fact which could perhaps be utilized in GCFR design to reduce reactivity from steam entry.

11. RELEVANCE TO GCFR DESIGN

Given the measured worths of simulated steam ingress in the Phase II GCFR assembly, despite the limitations of the critical experiments and their analysis, it is possible at this point to scope the potential reactivity problem from accidental steam entry in a real GCFR. To relate these Phase II data to steam worth in the 300 MW(e) design GCFR, several factors must be considered.

A first consideration is the maximum coolant steam density which could be reasonably expected from a steam generator leak. Conservative estimates from water inventories and other sources put this upper limit at about 1% water, or 10 g/ℓ H_2O, in the coolant. This is nearly equivalent in hydrogen content to the 8.8 g/ℓ CH_2 channel flooding in Phase II.

A second consideration is core size. A 3100-ℓ demonstration-size GCFR core could be expected to have a much more negative steam worth than this 1300-ℓ Phase II core. However, the fuel enrichments of both systems are roughly the same; the reason for the larger core is the larger void fraction (~60 vol % versus 44 vol %). This results in similar core k_∞ values and therefore similar leakage fractions in the neutron balances for both. Thus, the leakage-related positive components of core steam-flooding worth should be comparable in the Phase II and demonstration-plant GCFR designs.

Finally, at any time in the fuel cycle the GCFR core would be poisoned by either control rods or fission products. Also, the use of higher burnup plutonium (higher Pu-240 fraction) in the GCFR fuel rods would contribute more to the negative steam worth components.

In view of these factors, the flooding worths at 8.8 g/ℓ CH_2 in the near-critical rodded Phase II configuration should be a reasonable upper

bound for steam entry worth in a cold GCFR. Considering the last line of data in Table 2, it appears unlikely that 10 g/ℓ steam ingress into the coolant of a 300 MW(e) GCFR at low temperature could ever have a positive reactivity effect in excess of +60 Ih, or about +20¢.

At the operating temperature of a GCFR, the results of the uranium Doppler experiments (Ref. 17) in Phase II combined with the steam worth measurements provide an even more reassuring assessment of GCFR safety during a postulated steam leak accident. In the dry Phase II core, the measured central Doppler coefficient for depleted uranium was -0.623 Ih/kg for a temperature change of 300 to 1100 K. For the corresponding ΔT in the wet core (17.5 g/ℓ channel CH_2), the central coefficient almost doubled, to -1.197 Ih/kg of uranium.

Assuming center-to-average worth factors in the Phase II core of 2.20 radially and 1.60 axially (based on calculations), the core-average cold-to-hot Doppler effects would be -0.177 and -0.340 Ih/kg U-238, respectively, in the dry and wet configurations. A hypothetical heating of all the Phase II core U-238 (~2960 kg) would therefore reduce reactivity by 524 Ih for the dry configuration and by 1006 Ih for the wet configuration. The net effect for heating to a typical operating temperature, disregarding the Doppler in other materials (which should be more than compensated for by the omission of the blanket heating effects), would be a decrease of 482 Ih in the worth of 17.5 g/ℓ channel CH_2 flooding.

Thus, for a near critical Phase II core with 6$ of installed control rods and a temperature typical of a 300 MW(e) GCFR at power, CH_2 flooding at 17.5 g/ℓ in the voids (simulating about 2.2% steam) would have a reactivity effect of approximately -280 Ih, or about -0.87$. For a more realistic assessment of maximum uniform ingress of 1% steam, the reactivity effect would be negative by at least 0.44$, by a conservative linear interpolation.

12. SUMMARY

In summary, it is possible to adequately calculate the worths of simulated full core steam entry in a GCFR mockup by giving detailed attention to leakage parameters and to cross section averaging treatments and adjustments with hydrogen-moderated spectra. Worths of steam in a rodded core can be determined with the same accuracy as in a clean core provided that rod-shielding effects are re-evaluated at each steam density considered.

The complexities of the ZPR drawer loadings and the method of simulating steam introduce analytical uncertainties on the order of ± 50 Ih, on the basis of limited studies with heterogeneity modelling, for the full core flooding worths. Similar worth variations may be expected from future changes in methodology and basic nuclear data.

The analytical results have verified the experimentally identified sensitive correlations of steam worth with core geometry, steam density, and poison insertion. The studies also indicate a sensitivity to the size, as well as number and distribution, of the control rods. It would be appropriate to consider these sensitivities when designing the GCFR control rods to maximize rod worth enhancement in the event of steam ingress.

Experimental results from the simulated steam and Doppler worth measurements in the Phase II GCFR assembly have satisfactorily indicated that steam ingress at realistic density assumptions in a GCFR at typical operating conditions will have a negative reactivity input. However, the reactivity requirements of the control system may have to be increased slightly, on the order of 1$, as a contingency to cover the uncertainty of the effect of steam entry in a cold shutdown condition.

13. REFERENCES

1. "300 MW(e) Gas-Cooled Fast Breeder Reactor Demonstration Plant," General Atomic Report GA-A13045, July 1974.

2. Moore, R. A., "A Critical Experiment Program for the 300 MW(e) Gas Cooled Breeder Reactor - Scope and Purpose," USAEC Report Gulf-GA-A12780, Gulf General Atomic Company, October 1973.

3. Bhattacharyya, S. K., "An Experimental Study of the Neutronics of the First Gas Cooled Fast Reactor Benchmark Assembly (GCFR Phase I Assembly)," ERDA Report ANL-7636, Argonne National Laboratory, December 1976.

4. Hess, A. L., R. A. Rucker, and R. A. Moore, "Analysis of Steam Entry Experiment in the Phase I GCFR Critical Assembly," DOE Report GA-A14798, General Atomic Company, March 1978.

5. Pond, R. B., ed., "Reactor Physics Studies in the GCFR Phase II Critical Assembly," ERDA Report ANL 76-108, Argonne National Laboratory, September 1976.

6. Lathrop, K. D., and F. W. Brinkley, "TWOTRAN-II: An Interfaced Exportable Version of the TWOTRAN Code for Two-Dimensional Transport," USAEC Report LA-4848-MS, Los Alamos Scientific Laboratory, July 1973.

7. Merrill, M. H., "Nuclear Design Methods and Experimental Data in Use at Gulf General Atomic," General Atomic Report Gulf-GA-A12652, July 1973.

8. Mathews, D. R., et al., "GGC-5, A Computer Program for Calculating

Neutron Spectra and Group Constants," Gulf General Atomic Report GA-8871, September 1971.

9. Archibald, R. J., and D. R. Mathews, "The GAF/GAF/BAND Fast Reactor Cross Section Preparation System, Vol. II, GAND2 and GFE2, Computer Programs for Preparing Input Data for the GARGAR, GGC and MICROX Codes from an ENDF/B Format Nuclear Data File," USAEC Report GA-7542, Gulf General Atomic Company, March 1973.

10. Mathews, D. R., and P. K. Koch, "GANDY3, A Computer Program for the Evaluation of Effective Cross Sections in the Unresolved Resonance Region," USAEC Report GA-A12826, General Atomic Company, January 28, 1974.

11. Archibald, R., K. D. Lathrop, and D. Mathews, "1DFX-A Revised Version of the 1DF (DTF-IV) SN Transport Theory Code," Gulf General Atomic Report Gulf-GA-B10820, September 1971.

12. Benoist, P., "Streaming Effects and Collision Probabilities in Lattices," Nucl. Sci. Eng. 34, 285 (1968).

13. Kier, P., Argonne National Laboratory, private communication.

14. Wade, D. C., and E. M. Gelbard, "Neutron Streaming in Plate Criticals," Proceedings of the American Nuclear Society Topical Meeting on Advanced Reactors: Physics, Design, and Economics, CONF-740902, September 1974.

15. Little, W. W., Jr., and R. W. Hardie, "2DB User's Manual-Revision 1," Pacific Northwest Laboratory Report BNWL-831, Rev. 1, 1969.

16. Hardie, R. W., and W. W. Little, Jr., "PERT-V, A Two-Dimensional Perturbation Code for Fast Reactor Analysis," Pacific Northwest Laboratory Report BNWL-1162, September 1969.

17. Rucker, R. A., and A. L. Hess, "Evaluation of Central Doppler Worth in Simulated GCFR Configurations," Trans. Am. Nucl. Soc. 27, 949 (1977).

APPENDIX A
DETAILS OF PHASE II STEAM WORTH ANALYSIS

A.1. SPECIFICATIONS

The following tables and diagrams present the specifications used for the various spectrum, transport, and diffusion theory calculations involved in the GA analysis of the simulated steam flooding in the Phase II GCFR assembly. The data herein serve to document procedures at this stage of methods development and to give sufficient details to allow replication of the studies by other analysts or by future GA calculations using newer or revised codes.

Table A-1 gives pertinent data on the actual configurations of the Phase II assembly constructed on ZPR9 as part of the steam worth program. The listed core radii were derived on the basis of the as-loaded fissile-Pu mass and are the values used in the 2DB calculations. Experimental worths for steam flooding (Table 2 of text) were evaluated using the corrected loading reactivities in the last column of Table A-1.

Table A-2 presents input data for the GGC-5 cases used to prepare cross sections for the Phase II core cell with 17.5 g/ℓ channel CH_2 flooding. For the corresponding GGC-5 problems for the dry, 4.4, and 8.8 g/ℓ floodings, the CH_2 densities were reduced by factors of 0.000, 0.25, and 0.50. Each case represents a 4.143-cm wide region, or one quarter of the core three-drawer unit cell, encompassing a Pu-U-Mo (or U_3O_8) plate-column and its average associated diluents. The rodded-core case assumes that the B_4C is smeared over the three-drawer unit cell area, giving 1/4-column B_4C per Pu-U-Mo plate; this accounted for the influence of the B_4C on cross sections for the neighboring fuel plates. No rodded-core case was run with U_3O_8 as region 1, and the influence of the B_4C on the cross sections for U-238

TABLE A-1
LOADING AND REACTIVITY DATA FOR CONFIGURATIONS OF
PHASE II STEAM ENTRY STUDIES

Date	Loading Number	Fissile, Pu (kg) (±0.1%)	Effective Core Radius[a] (cm)	Averaged Steam Ingress (g/cc CH_2 in Void Channels)	No. of B_4C Rods Inserted	Assembly Reactivity (Ih)	
						Measured as of Run Date	Corrected for Pu-241 Decay[b]
1-6-76	65	589.45	56.813	--	--	22.0 ± 0.2	22.0 ± 0.2
1-7-76	66	590.78	56.877	--	--	66.4 ± 0.5	66.6 ± 0.5
1-22-76	72	548.20	54.789	--	--	-1353.6 ± 9	-1351.0 ± 9
1-30-76	76	548.20	54.789	0.0044	--	-1268.4 ± 4	-1264.5 ± 4
2-10-76	80	548.20	54.789	0.0088	--	-1146.0 ± 11	-1140.3 ± 11
2-11-76	81	574.86	56.105	0.0088	--	-247.6 ± 1.2	-241.7 ± 1.2
2-12-76	82	574.86	56.105	0.0088	1	-746.9 ± 3.9	-740.8 ± 3.9
2-13-76	83	584.47	56.621	0.0088	--	-77.6 ± 0.2	+83.8 ± 0.2
3-10-76	96	548.20	54.789	0.0175	--	-823.9 ± 3.6	-813.4 ± 3.6
3-11-76	97	569.49	55.843	0.0175	--	-141.0 ± 0.9	-130.3 ± 1.0
4-20-76	112	577.50	56.234	0.0175	--	+129.5 ± 0.2	+146.7 ± 0.2
4-21-76	113	577.50	56.234	0.0175	1	-415.3 ± 3.7	-397.9 ± 3.7
4-22-76	114	577.50	56.234	0.0175	8	-1932 ± 33	-1914 ± 33
5-5-76	117	630.71	58.768	0.0175	8	-461.4 ± 3.5	-441.7 ± 3.5
5-6-76	118	644.00	59.384	0.0175	8	-116.9 ± 1.0	-97.1 ± 1.0
5-11-76	126	644.00	59.384	0.0088	8	-290.7 ± 1.5	-270.0 ± 1.5
5-14-76	133	644.00	59.384	--	8	-320.3 ± 1.5	-299.1 ± 1.5
5-18-76	134	577.50	56.234	--	8	-2293 ± 34	-2271 ± 34
5-19-76	135	577.50	56.234	--	1	-843.5 ± 4.2	-821.5 ± 4.2
5-14-76	136	577.50	56.234	--	--	-359.3 ± 1.8	-337.3 ± 1.8

[a] Based on volume, determined from fissile mass and cell-averaged fissile density of 476.195 g/ℓ and core length of 122.07 cm.

[b] Corrected to reference date (1-6-76) using decay worth of -0.164 ± 0.015 Ih/day.

TABLE A-2
SPECIFICATIONS FOR GGC-5 PROBLEMS TO GENERATE
PHASE II CORE CROSS SECTIONS

Set No. - Cell Type		A - Core Fuel		B - Core Oxide		C - Rodded Core	
GGC-5 Region No.		1	2	1	2	1	2
Region Contents		Pu-U-Mo Plate	Diluents + U_3O_8	U_3O_8 Plate	Diluents + Fuel	Pu-U-Mo Plate	Diluents U_3O_8, B_4C
Region Thickness (cm)		0.5100	0.36334	0.5990	3.5444	0.5100	3.36334
Density (10^{21}/cm^3):							
H[a]		--	0.6108	--	0.6261	--	0.5062
C[a]		--	0.3054	--	0.3131	--	2.0342
B-10		--	--	--	--	--	1.3599
B-11		--	--	--	--	--	5.5141
O		--	15.3291	40.5910	8.8538	--	15.3384
Cr		--	3.2874	--	3.3700	--	3.2925
Mn		--	0.2577	--	0.2642	--	0.2608
Fe		--	17.5115	--	17.9512	--	17.5335
Ni		--	1.5145	--	1.5526	--	1.5177
Mo		2.5356	--	--	0.3648	2.5356	--
U-235		0.0606	0.0054	0.0320	0.0088	0.0606	0.0054
U-238		27.1197	2.5134	15.2122	3.9078	27.1197	2.5134
Pu-239		9.6126	--	--	1.3832	9.6126	--
Pu-240		1.2747	--	--	0.1834	1.2747	--
Pu-241		0.1324	--	--	0.0191	0.1324	--
Pu-242		0.0187	--	--	0.0027	0.0187	--
Am-241		0.0755	--	--	0.0109	0.0755	--
Region 1 Dancoff Factor[b] C-resol	Dry	0.1194		0.1060		0.0945	
	4.4 g/ℓ CH_2	0.1176		0.1044		--	
	8.8 g/ℓ CH_2	0.1155		0.1026		0.0921	
	17.5 g/ℓ CH_2	0.1121		0.0996		0.0897	
Region 1 Effective Scatter Σ_m-unr[c]	Dry	1.271		0.9910		1.328	
	4.4 g/ℓ CH_2	1.276		0.9944		--	
	8.5 g/ℓ CH_2	1.280		0.9980		1.333	
	17.5 g/ℓ CH_2	1.288		1.004		1.339	

[a] For 17.5 g/ℓ channel CH_2 flooding.

[b] For resolved resonance range (GAROL routine).

[c] For unresolved resonance integrals (GANDY), to evaluate scattering per absorber atom: $\Sigma_m = \Sigma N_i \cdot \sigma_i + (1 - C_{unr})/2t$.

in U_3O_8 was assumed to be similar to the changes to the U-238 cross sections for the Pu-U-Mo plate (comparing case 3 versus case 1 outputs). For all three cell cases, separate input and output data streams were maintained for the U-238 cross sections in the two types of plates (Pu-U-Mo and U_3O_8). The lower section of Table A-2 lists other input data for the flooded and dry-core GGC-5 runs pertaining to the heterogeneity effects on resonance cross section averaging. Spatial dependence of flux was represented by input bucklings on a 28-group energy mesh.

Table A-3 gives the 28-group structure and lists the buckling values used for the clean core cells without flooding (dry) and with 17.5 g/ℓ CH_2 (wet); bucklings for the intermediate floodings were linear interpolations of the wet and dry sets. Different sets were used for the rodded cells to include inleakage to the three-drawer rodded region. All of the selected buckling sets were derived from previous 2DB calculations for the Phase II system using earlier models and cross section methods.

Table A-4 gives the input specifications for the blanket and reflector region GGC-5 cases. For the two-region model of the blanket zone cells, region 1 represented (in dimensions and composition) the average clustering of fertile material plates. Input bucklings provided for inleakage from the core to the blanket zones. For the reflector GGC-5, an average homogeneous composition for the radial and axial reflectors was used and a minute content of fissionable material was included, for which the input fission spectrum represented that of a source equivalent to the blanket-to-reflector inleakage.

Table A-5 summarizes some of the basic output information from the spectrum code calculations, the 1-group collapsed values of microscopic cross sections, and the derived reactivity parameters for the specific cells. Although a highly oversimplified reactor representation, these data do indicate the relative effects of the increased density steam floodings on average fission, capture, and transport cross sections. For the core, k_∞ values decrease with added CH_2, but an average buckling (representing a critical dry system) produces k-effective values which increase with added CH_2.

TABLE A-3
ENERGY STRUCTURE AND SPECTRA FOR PHASE II GCFR ASSEMBLY ANALYSIS

Group No.[a]	Lower Energy Boundary[b] (eV)	Fission Spectrum (%)	2DB Spectra at Core Center (%)		Input Bucklings (B^2) for GGC-5 (10^{-4} cm^{-2})	
			Dry	17.5 g/ℓ Channel CH_2	Dry Core	Core with 17.5 g/ℓ CH_2 in Channels
1	1.000+07	0.234	0.0250	0.0270	24.14	24.15
2	6.056+06	3.072	0.342	0.370	24.23	24.30
3	3.679+06	11.837	1.371	1.483	25.04	25.25
4	2.231+06	20.876	3.523	3.773	22.69	22.89
5	1.353+06	22.317	5.005	5.329	22.08	22.32
6	8.209+05	17.416	6.845	7.170	19.99	20.18
7	4.979+05	11.182	13.231	13.178	15.52	15.93
8	3.020+05	6.369	10.280	10.044	15.30	15.41
9	1.832+05	3.371	12.077	11.319	12.85	13.19
10	1.111+05	1.706	11.586	10.359	12.15	12.45
11	6.738+04	0.840	9.500	8.229	10.33	10.83
12	4.087+04	0.407	7.675	6.591	8.966	9.502
13	2.479+04	0.195	4.869	4.438	3.442	5.037
14	1.503+04	0.0931	5.237	4.855	10.28	11.31
15	9.119+03	0.0442	3.251	3.360	6.249	7.907
16	5.531+03	0.0210	1.660	2.098	0.0611	4.838
17	3.555+03	9.92-03	1.392	2.015	5.258	8.028
18	2.035+03	4.69-03	0.911	1.552	0.3988	4.429
19	1.234+03	2.22-03	0.628	1.296	-2.700	3.278
20	7.485+02	1.05-03	0.308	0.826	-14.690	-3.511
21	4.540+02	4.95-04	0.163	0.603	-23.48	-6.559
22	2.754+02	2.34-04	0.0672	0.359	-46.33	-17.43
23	1.013+02	1.63-04	0.0485	0.461	-86.94	-29.98
24	3.727+01	3.63-05	4.89-03	0.146	-304.90	-87.82
25	1.371+01	8.10-06	5.19-04	0.0688	-487.3	-64.60
26	5.054+00	1.81-06	4.01-05	0.0248	-635.9	-117.1
27	1.855+00	4.01-07	5.20-06	0.0185	-295.9	-43.92
28	4.140-01	1.02-07	1.85-06	6.89-03	-1504.1	-428.9

[a] Underlining indicates 10-group boundaries.

[b] Upper boundary for group 1 at 14.92 MeV (lethargy = -0.40).

TABLE A-4
SPECIFICATIONS FOR GGC-5 PROBLEMS TO GENERATE
PHASE II BLANKET CROSS SECTIONS

Set No. - Region Cell		D - Radial Blanket		E - Axial Blanket		F - Reflector
GGC-5 Region No.		1	2	1	2	1 and 2
Region Contents		Depleted U + U_3O_8	Steel (+ CH_2)	Depleted U + U_3O_8	Steel (+ CH_2)	Steel Blocks
Region Thickness (cm)		1.3568	1.4055	0.9112	1.1605	5.5245
Density (10^{21}/cc):						
H		--	0.9371[a]	--	0.9562[a]	--
C		--	0.4685[a]	--	0.4781[a]	0.2267
O		36.2384	0.3803	33.1514	0.3449	--
Si		--	--	--	--	1.0358
Cr		--	4.9304	--	4.4849	15.4217
Mn		--	0.3821	--	0.3471	1.4130
Fe		--	17.3343	--	15.7676	54.2475
Ni		--	2.2352	--	2.0398	6.7351
Mo		--	0.0195	--	0.0173	0.0393
U-235		0.0395	--	0.0423	--	--
U-238		18.5089	--	19.7786	--	1.00-07
Region 1 Dancoff Factor[b] C-resol	Dry	0.4367		0.5278		--
	4.4 g/ℓ CH_2	0.4320		0.5230		--
	8.8 g/ℓ CH_2	0.4275		0.5176		--
	17.5 g/ℓ CH_2	0.4185		0.5086		--
Region 1 Effective Scatter Σ_m-unr[c]	Dry	0.5254		0.5566		--
	4.4 g/ℓ CH_2	0.5280		0.5604		--
	8.8 g/ℓ CH_2	0.5306		0.5646		--
	17.5 g/ℓ CH_2	0.5358		0.5714		--

[a] For 17.5 g/ℓ channel CH_2 flooding.

[b] For resolved resonance range.

[c] For unresolved resonance integrals: $\Sigma_m = \Sigma N_i \cdot \sigma_i + (1 - C_{unr})/2t$.

TABLE A-5
SUMMARY OF PHASE II GGC-5 OUTPUT DATA

Set No.	Cell Type	1-Group Parameters	Void Channel CH_2 Flooding (g/ℓ)			
			Dry	4.4	8.8	17.5
A	Core Fuel; Pu-U-Mo in Region 1	$\nu\Sigma_f$	0.007180	0.007385	0.007600	0.007915
		Σ_{abs}-Σ_{n2n}	0.004586	0.004796	0.005013	0.005324
		Σ_{tr}	0.16158	0.16327	0.16463	0.16643
		Avg. DB^2(a)	0.002768	0.002755	0.002749	0.002802
		k-infinity	1.5655	1.5398	1.5159	1.4867
		k-effective(a)	0.9762	0.9779	0.9790	0.9739
		adjusted k(b)	1.0000	1.0030	0.0054	1.0092
B	Core Oxide: U_3O_8 in Region 1	$\nu\Sigma_f$	0.007188	0.007394	0.007615	0.007985
		Σ_{abs}-Σ_{n2n}	0.004590	0.004796	0.005012	0.005339
		Avg. DB^2(a)	0.002781	0.002778	0.002780	0.002827
		k-infinity	1.5658	1.5417	1.5193	1.4907
		k-effective	0.9751	0.9762	0.9772	0.9745
		adjusted k(b)	1.0000	1.0034	1.0065	1.0120
C	Rodded Core: Pu-U-Mo in Region 1; B_4C, etc. in Region 2	$\nu\Sigma_f$	0.007129	--	0.007327	0.007495
		Σ_{abs}-Σ_{n2n}	0.006859	--	0.007338	0.007720
		Σ_{tr}	0.20710	--	0.22338	0.22797
		Avg. DB^2(a)	0.000572	--	0.000233	0.000127
		k-infinity	1.03926	--	0.9986	0.9709
		k-effective	0.9592	--	0.9679	0.9551
		adjusted k(b)	0.8025	--	0.7953	0.7842
D	Radial Blanket	$\nu\Sigma_f$	5.332-04	5.561-04	5.864-04	6.334-04
		Σ_{abs}-Σ_{n2n}	3.694-03	3.880-03	4.038-03	4.289-03
		Σ_{tr}	0.18048	0.18074	0.18113	0.18370
		Avg. DB^2(a)	-2.725-03	-2.887-03	-2.998-03	-3.177-03
		k-infinity	0.1443	0.1433	0.1452	0.1477
		k-effective(a)	0.5497	0.5581	0.5600	0.5601
E	Axial Blanket	$\nu\Sigma_f$	5.125-04	5.430-04	5.820-04	6.233-04
		Σ_{abs}-Σ_{n2n}	3.338-03	3.543-04	3.653-04	3.970-03
		Σ_{tr}	0.16487	0.16511	0.16453	0.16449
		Avg. DB^2(a)	-2.391-03	-2.551-03	-2.586-03	-2.842-03
		k-infinity	0.1535	0.1533	0.1594	0.1570
		k-effective(a)	0.5413	0.5476	0.5419	0.5436

(a) As determined using input bucklings

(b) Using adjusted average B^2 = 0.001257

Table A-6 gives compositions used for the DTFX cell calculations, including the various fuel, fertile, and diluent plate columns, the mockup B_4C rod, and the void channels with and without 17.5 g/ℓ CH_2 ingress. The horizontal structure of the ZPR9 (matrix top and bottom and drawer bottom) has been smeared into the void channels, vertical matrix, fuel and void clads, and Fe_2O_3 columns.

Table A-7 provides the geometric details of the DTFX models, in this case with the B_4C mockup rod column near the center of the three-drawer core cell; for the clean cell cases, the STB/ROD/STB material combination was replaced by STV/VOI/STV, using the material symbols as defined in Table A-6. Because of the equivalent chord modelling for the fuel plates, the DTFX three-drawer cell geometry is distorted from the physical dimensions (5.5245 x 16.5735 cm), but overall the cell average compositions are preserved.

Tables A-8 and A-9 give composition and geometric details, respectively, for the TWOTRAN model of the rodded Phase II core cell with 17.5 g/ℓ CH_2 flooding in the void channels (see also Fig. 2 of the main text). For the unrodded cell, only the Y-direction regions 4 and 5 (Table A-9) were modeled, giving 10 Y-direction mesh intervals and 50 X-direction intervals. In the dry cases, with and without the B_4C rod, the H and C contributions from CH_2 for materials QUO and HUO (Table A-8) were deleted.

Input cross sections for the various material plate regions in the DTFX and TWOTRAN problems were as provided by the appropriate core cell GGC-5 cases; for the resolved resonance materials (fuel and U_3O_8), in-plate cross sections were derived from the GAROL two-region cell average data by applying inverse shielding factors, i.e., using the GGC-5 output cross sections (groups 16 to 28) multiplied by the cell average/region-1 flux ratios edited by the code.

Figure A-1 presents geometric and mesh details of the 2DB model used for the flooding configurations of Phase II. Region compositions for the calculations are as given in Tables A-10 and A-11 for the full flooding, 17.5 g/ℓ CH_2 cases; the C and H densities for the core blanket regions were

TABLE A-6
COMPOSITIONS FOR DTFX MODEL OF PHASE II CORE CELL

Region Material	Pu-U-Mo Fuel Plate	Fuel Clad	Iron Oxide (Fe_2O_3)	U-oxide (U_3O_8)	Matrix Steel	Void-Can Steel Clad	Void Channel	Flooded Channel (17.5 g/ℓ CH_2)	B_4C[(a)] Mockup Rod	B_4C Rod Clad
Symbol	PUM	STF	FEO	UOX	STM	STV	VOI	CH2	ROD	STB
10^{21} n/cc										
CH_2-H	--	--	--	--	--	--	--	1.3054	--	--
CH_2-C	--	--	--	--	--	--	--	0.6527	--	--
B_4C-B-10	--	--	--	--	--	--	--	--	14.8094	--
B_4C-B-11	--	--	--	--	--	--	--	--	60.0579	--
C	--	--	--	--	--	--	--	--	19.0078	--
0	--	1.6884	51.0722	39.2866	2.0296	1.5273	0.2213	0.2213	0.7049	3.2377
Cr	--	10.9011	1.1908	--	13.0637	11.6940	1.4297	1.4297	--	22.6108
Mn	--	0.9241	0.0948	--	1.0577	0.8786	0.1126	0.1126	--	1.9389
Fe	--	37.6560	39.7592	--	46.6569	40.8273	5.0754	5.0754	--	86.1516
Ni	--	5.3772	0.5182	--	5.6935	5.9001	0.6406	0.6406	--	11.0209
Mo	2.5364	--	--	--	--	--	--	--	--	--
U-235	0.0612	--	--	0.0327	--	--	--	--	--	--
U-238	27.9428	--	--	14.845	--	--	--	--	--	--
U-239	9.9302	--	--	--	--	--	--	--	--	--
Pu-240	1.3161	--	--	--	--	--	--	--	--	--
Pu-241	0.1334	--	--	--	--	--	--	--	--	--
Pu-242	0.0192	--	--	--	--	--	--	--	--	--
Am-241	0.0814	--	--	--	--	--	--	--	--	--

(a) Actual density x mass/surface factor of 0.8048.

TABLE A-7
SPECIFICATIONS FOR DTFX MODEL OF PHASE II RODDED CORE CELL

Region No.	Material Symbol[a]	Region Width[b] (cm)	Coordinate (cm)	No. Mesh Spaces	Region No.	Material Symbol	Region Width (cm)	Coordinate (cm)	No. Mesh Spaces
			0.0000						
1	STM	0.2292	0.2292	1	27	UOX	0.6350	9.1798	3
2	UOX	0.6350	0.8642	3	28	STV	0.0578	9.2376	1
3	STV	0.0578	0.9220	1	29	VOI	0.5589	9.7965	1
4	VOI	0.5589	1.4809	1	30	STV	0.0578	9.8543	1
5	STV	0.0578	1.5387	1	31	FEO	0.3175	10.1718	2
6	FEO	0.3175	1.8562	2	32	STF	0.0823	10.2541	1
7	STF	0.0823	1.9385	1	33	PUM	0.5100	10.7641	4
8	PUM	0.5100	2.4485	4	34	STF	0.0823	10.8464	1
9	STF	0.0823	2.5308	1	35	FEO	0.3175	11.1639	2
10	FEO	0.3175	2.8483	2	36	STM	0.4583	11.6222	3
11	STV	0.0578	2.9060	1	37	STV	0.0578	11.6800	1
12	VOI	1.1940	4.1000	2	38	VOI	1.1940	12.8740	2
13	STV	0.0578	4.1578	1	39	STV	0.0578	12.9318	1
14	UOX	0.6350	4.7928	3	40	UOX	0.6350	13.5668	3
15	STV	0.0578	4.8506	1	41	STV	0.0578	13.6246	1
16	VOI	0.5589	5.4095	1	42	VOI	0.5589	14.1835	1
17	STV	0.0578	5.4673	1	43	STV	0.0578	14.2413	1
18	STM	0.4583	5.9256	3	44	FEO	0.3175	14.5588	2
19	FEO	0.3175	6.2431	2	45	STF	0.0823	14.6411	1
20	STF	0.0823	6.3254	1	46	PUM	0.5100	15.1511	4
21	PUM	0.5100	6.8354	4	47	STF	0.0823	15.2334	1
22	STF	0.0823	6.9177	1	48	FEO	0.3175	15.5509	2
23	FEO	0.3175	7.2352	2	49	STV	0.0578	15.6097	1
24	STB	0.0578	7.2930	1	50	VOI	1.1940	16.8027	2
25	ROD	1.1940	8.4970	6	51	STV	0.0578	16.8605	1
26	STB	0.0578	8.5448	1	52	STM	0.2292	17.0897	1

[a] As defined in Table A-2.

[b] Assumed height of 5.3576 cm for cell.

TABLE A-8
COMPOSITIONS USED FOR PHASE II TWOTRAN CALCULATIONS
(10^{21} atoms/cm^3)

Cell Region	Pu-U-Mo Fuel Plate	Uranium Oxide (U_3O_8)	Fe_2O_3 Plus Fuel Clad	Matrix Plus Drawer Smear	Flooded 1/4-in. Channel Plus Homogenized Clad	Flooded 1/2-in. Channel Plus Homogenized Clad	Mockup Control Rod	B_4C Clad
Symbol	PUU	UOX	FEX	MTX	QVO	HVO	B4C	BST
CH_2-H	--	--	--	--	1.2135	1.2959	--	--
CH_2-C	--	--	--	--	0.6068	0.6480	--	--
B-10	--	--	--	--	--	--	18.4013	--
B-11	--	--	--	--	--	--	74.6245	--
C	--	--	--	--	--	--	23.6181	--
O	--	41.5766	45.1784	1.8634	0.2847	0.1584	0.8759[a]	2.8810
Cr	--	--	2.2172	11.8378	2.2373	1.2446	--	22.6419
Mn	--	--	0.1894	0.9518	0.1670	0.0929	--	1.6896
Fe	--	--	38.9258	42.2368	7.7930	4.3353	--	78.8655
Ni	--	--	1.1110	5.1558	1.1464	0.6378	--	11.6018
Mo	2.6751	--	--	--	--	--	--	--
U-235	0.0646	0.0346	--	--	--	--	--	--
U-238	29.4702	15.7066	--	--	--	--	--	--
Pu-239	10.4730	--	--	--	--	--	--	--
Pu-240	1.3880	--	--	--	--	--	--	--
Pu-241	0.1407	--	--	--	--	--	--	--
Pu-242	0.0203	--	--	--	--	--	--	--
Am-241	0.0858	--	--	--	--	--	--	--

[a] Representing Si.

TABLE A-9
SPECIFICATIONS FOR TWOTRAN MODEL OF
3 x 3 DRAWER RODDED CORE CELL FOR PHASE II

X-Direction Specifications			Y-Direction Specifications and Materials[a]				
			1	2	3	4	5
Region No.	Upper Boundary (cm)	No. of Mesh Spaces	2.5400 9 Mesh Spaces	2.9845 2 Mesh Spaces	5.5245 9 Mesh Spaces	8.0645 9 Mesh Spaces	8.2868 2 Mesh Spaces
29	16.5735	2	UOX	MTX	UOX	UOX	MTX
28	15.9385	1	QVO	MTX	QVO	QVO	MTX
27	15.3035	1	FEC	MTX	FEC	FEC	MTX
26	14.9235	3	PUU	MTX	PUU	PUU	MTX
25	14.4135	1	FEC	MTX	FEC	FEC	MTX
24	14.0335	2	HVO	MTX	HVO	HVO	MTX
23	12.7635	2	UOX	MTX	UOX	UOX	MTX
22	12.1285	1	QVO	MTX	QVO	QVO	MTX
21	11.4935	2	MTX	MTX	MTX	MTX	MTX
20	11.0490	1	FEC	MTX	FEC	FEC	MTX
19	10.6690	3	PUU	MTX	PUU	PUU	MTX
18	10.1590	1	FEC	MTX	FEC	FEC	MTX
17	9.7790	1	BST	MTX	HVO	HVO	MTX
16	9.7741	4	B4C	MTX	HVO	HVO	MTX
15	8.5470	1	BST	MTX	HVO	HVO	MTX
14	8.5090	2	UOX	MTX	UOX	UOX	MTX
13	7.8740	1	QVO	MTX	QVO	QVO	MTX
12	7.2390	1	FEC	MTX	FEC	FEC	MTX
11	6.8590	3	PUU	MTX	PUU	PUU	MTX
10	6.3490	1	FEC	MTX	FEC	FEC	MTX
9	5.9690	2	MTX	MTX	MTX	MTX	MTX
8	5.5245	2	HVO	MTX	HVO	HVO	MTX
7	4.2545	2	UOX	MTX	UOX	UOX	MTX
6	3.6195	1	QVO	MTX	QVO	QVO	MTX
5	2.9845	1	FEC	MTX	FEC	FEC	MTX
4	2.6045	3	PUU	MTX	PUU	PUU	MTX
3	2.0945	1	FEC	MTX	FEC	FEC	MTX
2	1.7145	2	HVO	MTX	HVO	HVO	MTX
1	0.0445	2	MTX	MTX	MTX	MTX	MTX
0	0.0000						

[a] Material compositions as given in Table A-8.

* Dashed-line border indicates area for averaging flux-advantage factors.

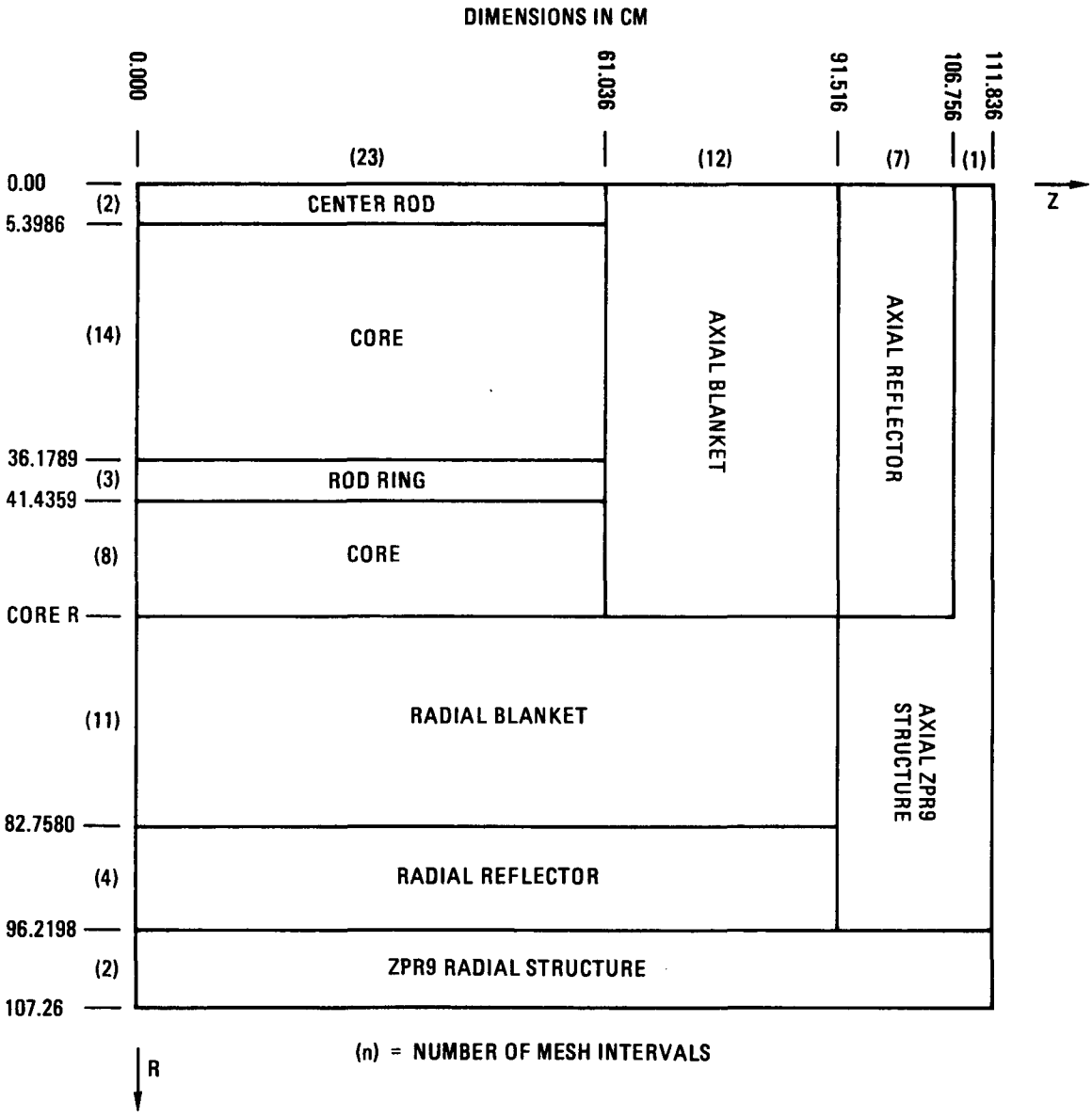

Fig. A-1. Geometric model of Phase II GCFR assembly for R-Z diffusion theory calculations

TABLE A-10
COMPOSITIONS USED FOR CORE AND MOCKUP ROD REGIONS IN PHASE II 2DB DIFFUSION CALCULATIONS

Materials	Compositions (10^{21} atoms/cm^3)		
	Normal Core With 17.5 g/ℓ Channel CH_2	Central B_4C Rod With 17.5 g/ℓ Channel CH_2	Outer Ring B_4C Rods With 17.5 g/ℓ Channel CH_2
B_4C			
B-10	--	1.1933	0.5966
B-11	--	4.8393	2.4196
C	--	1.5316	0.7658
O[a]	--	0.0568	0.0284
CH_2			
H[b]	0.5356	0.4444	0.4900
C[b]	0.2678	0.2222	0.2450
Std. Core			
C	0.0303	0.0606	0.0454
O	13.6285	13.6397	13.6341
Cr	2.8828	2.8814	2.8821
Mn	0.2260	0.2273	0.2266
Fe	15.3562	15.3993	15.3778
Ni	1.3281	1.3287	1.3284
Mo	0.3121	0.3121	0.3121
Total U-235	0.0122	0.0122	0.0122
Alloy U-238	3.3314	3.3314	3.3314
Oxide U-238	2.2107	2.2107	2.2107
Pu-239	1.1839	1.1839	1.1839
Pu-240	0.1569	0.1569	0.1569
Pu-241	0.0159	0.0159	0.0159
Pu-242	0.0023	0.0023	0.0023
Am-241	0.0097	0.0097	0.0097

[a] Used to represent Si and other impurities in B_4C.

[b] These densities' time factors of 0.000, 0.2500 and 0.5065 were used for dry, 4.4 g/ℓ, and 8.8 g/ℓ CH_2 average channel density cases, respectively.

TABLE A-11
COMPOSITIONS USED FOR BLANKET AND REFLECTOR REGIONS IN PHASE II CALCULATIONS

Material	Compositions (10^{21} atoms/cm^3)					
	Radial Blanket With 17.5 g/ℓ Channel CH_2	Axial Blanket With 17.5 g/ℓ Channel CH_2	Radial Reflector	Axial Reflector	ZPR9 Radial Structure	ZPR9 Axial Structure
CH_2						
H[a]	0.4769	0.5356	--	--	--	--
C[a]	0.2384	0.2678	--	--	--	--
Dry						
C	0.0281	0.0278	0.2164	0.2370	0.0057	0.0021
O	17.9648	14.7473	--	--	--	--
Si	--	--	0.9834	1.0881	0.2948	0.1081
Cr	2.5087	2.5122	15.7448	15.0985	4.9091	1.8000
Mn	0.1944	0.1944	1.3752	1.4507	0.4018	0.1473
Fe	8.8201	8.8321	55.5996	52.8953	17.2449	6.3231
Ni	1.1373	1.1426	6.7956	6.6746	2.1856	0.8014
Mo	0.0099	0.0097	0.0730	0.0550	0.0216	0.0079
U-235	0.0194	0.0186	--	--	--	--
U-238	9.0911	8.6998	--	--	--	--

[a] For intermediate flooding, 8.8 and 4.4 g/ℓ CH_2 densities reduced by factors 0.5065 and 0.250.

proportionately reduced for the intermediate density and dry cases. The cross sections for the 2DB core regions were those previously used (but in diffusion code format) for the DTFX calculations (inplate data by material) with, however, the DTFX (or TWOTRAN) output cell flux factors applied as heterogeneity corrections over the full energy range. For the 2DB blanket regions, the cross section used were taken directly from the blanket GGC-5 cases.

A.2. DIFFUSION MODIFIERS

Neutron streaming, through void channels used in the ZPR9 assemblies to mock up the GCFR coolant fraction, was provided by anisotropic diffusion coefficients in the diffusion theory calculations. Directional modifiers, M, produced by the Benoist theory code PLADIF were used so that the anisotropic diffusion coefficients were obtained as the product of the Benoist modifiers and the normal isotropic diffusion coefficient $1/3\Sigma_{tr}$. For the directions parallel to the void slots

$$D_{\parallel} = M_{\parallel} /3\Sigma_{tr} \quad ,$$

whereas for the direction perpendicular to the slots

$$D_{\perp} = M_{\perp}/3\Sigma_{tr} \quad .$$

In the R-Z model the parallel and perpendicular results were arithmetically averaged for use in the R directions:

$$D_R = (D_{\parallel} + D_{\perp})/2 \quad .$$

The 10- and 28-group multipliers $M_{\perp}$ and $M_{\parallel}$ were generated for three basic unit cells with and without CH_2 ingress: (1) the core three-drawer unit cell, (2) the axial blanket three-drawer unit cell, and (3) the radial blanket unit cell, using the PLADIF formula

$$\frac{M_k}{(\Sigma_{tr})_{cell}} = \frac{\sum_i \sum_j V_i \phi_i \frac{1}{(\Sigma_{tr})_j} P_{ij,k}}{\sum_i V_i \phi_i} \quad .$$

Here V_i, ϕ_i, and $(\Sigma_{tr})_j$ are, respectively, the width, average flux, and macroscopic transport cross section in plate i of the cell, and

$$P_{ij,k} = \frac{3(\Sigma_{tr})_j}{V_i} \int_{V_j} d\vec{r} \int_{V_i} d\vec{r} \frac{e^{-\Sigma|\vec{r} - \vec{r}'|}}{4\pi|\vec{r} - \vec{r}|^2} \Omega_k^2$$

is the directional probability that source neutrons in plate i suffer their first collision in region j. Here Ω_k is the direction cosine, and k = || or k = $\perp$.

Tables A-12 and A-13 list the radial and axial diffusion modifiers generated by PLADIF with half-cell descriptions for the dry and wet (17.5 g/ℓ CH_2 in voids) cores, respectively, to be used in the 28-group 2DB calculations. For intermediate flooding calculations, interpolations between the dry and wet modifiers were used.

Tables A-14 and A-15 list the results of the 10- and 28-group 2DB calculations for the various configurations of the steam flooding experiments. For the 10-group cases (Table A-14), the data include comparative eigenvalues obtained with DTFX- and TWOTRAN-generated heterogeneity factors. In the 28-group results, the effects of lumping versus smearing the CH_2 at the intermediate density floodings are compared.

Table A-16 summarizes the results of calculations using the PERT code for effective delayed neutron parameters and reactivity conversion factors for the Phase II dry and wet configurations. For the 4.4 and 8.8 g/ℓ CH_2 density loadings, interpolations between dry and wet conversion factors were used to relate calculated eigenvalues to reactivity in Ih or dollars.

TABLE A-12
RADIAL MODIFIERS FOR PHASE II DIFFUSION COEFFICIENTS

	Core		Radial Blanket		Axial Blanket	
	Dry	Wet	Dry	Wet	Dry	Wet
1	1.0548	1.0540	1.0126	1.0121	1.0172	1.0164
2	1.0551	1.0543	1.0124	1.0120	1.0168	1.0161
3	1.0558	1.0546	0.0142	1.0134	1.0192	1.0180
4	1.0494	1.0480	0.0149	1.0139	1.0201	1.0186
5	1.0492	1.0474	1.0198	1.0184	1.0263	1.0243
6	1.0573	1.0540	1.0376	1.0350	1.0449	1.0412
7	1.0495	1.0466	1.0292	1.0262	1.0369	1.0327
8	1.0770	1.0711	1.0588	1.0542	1.0685	1.0622
9	1.0705	1.0659	1.0442	1.0399	1.0558	1.0497
10	1.0734	1.0664	1.0470	1.0419	1.0599	1.0526
11	1.0805	1.0724	1.0456	1.0405	1.0600	1.0527
12	1.0852	1.0751	1.0483	1.0425	1.0635	1.0554
13	1.1011	1.0903	1.0413	1.0376	1.0555	1.0500
14	1.0804	1.0684	1.0548	1.0475	1.0710	1.0608
15	1.0842	1.0716	1.0462	1.0408	1.0625	1.0546
16	1.1000	1.0938	1.0520	1.0487	1.0628	1.0578
17	1.0942	1.0819	1.0475	1.0434	1.0620	1.0563
18	1.0992	1.0852	1.0476	1.0438	1.0621	1.0564
19	1.0997	1.0844	1.0437	1.0390	1.0594	1.0522
20	1.1041	1.0851	1.0426	1.0383	1.0565	1.0501
21	1.1061	1.0859	1.0406	1.0365	1.0541	1.0479
22	1.1138	1.0933	1.0605	1.0599	1.0656	1.0630
23	1.1165	1.0926	1.0451	1.0410	1.0599	1.0541
24	1.1198	1.0844	1.0399	1.0365	1.0517	1.0469
25	1.1044	1.0684	1.0425	1.0381	1.0558	1.0488
26	1.1079	1.0579	1.0405	1.0370	1.0525	1.0473
27	1.0990	1.0679	1.0381	1.0347	1.0473	1.0422
28	1.1336	1.0712	1.0389	1.0356	1.0484	1.0433

TABLE A-13
AXIAL MODIFIERS FOR PHASE II DIFFUSION COEFFICIENTS

	Core		Radial Blanket		Axial Blanket	
	Dry	Wet	Dry	Wet	Dry	Wet
1	1.0775	1.0757	1.0245	1.0235	1.0336	1.0321
2	1.0789	1.0769	1.0240	1.0231	1.0327	1.0313
3	1.0825	1.0797	1.0273	1.0258	1.0323	1.0350
4	1.0781	1.0743	1.0286	1.0266	1.0390	1.0359
5	1.0830	1.0784	1.0380	1.0353	1.0508	1.0468
6	1.1041	1.0963	1.0718	1.0667	1.0862	1.0788
7	1.0915	1.0837	1.0558	1.0501	1.0709	1.0627
8	1.1443	1.1309	1.1100	1.1010	1.1292	1.1668
9	1.1308	1.1186	1.0828	1.0745	1.1053	1.0934
10	1.1377	1.1217	1.0877	1.0778	1.1126	1.0984
11	1.1485	1.1315	1.0840	1.0743	1.1118	1.0977
12	1.1565	1.1369	1.0888	1.0775	1.1181	1.1024
13	1.1785	1.1604	1.0721	1.0652	1.1003	1.0898
14	1.1517	1.1282	1.1008	1.0868	1.1321	1.1122
15	1.1549	1.1331	1.0834	1.0732	1.1147	1.0998
16	1.1740	1.1651	1.0842	1.0785	1.1085	1.0994
17	1.1663	1.1473	1.0804	1.0730	1.1099	1.0992
18	1.1753	1.1543	1.0804	1.0734	1.1099	1.0991
19	1.1809	1.1569	1.0767	1.0682	1.1075	1.0940
20	1.1877	1.1608	1.0735	1.0657	1.1014	1.0895
21	1.1923	1.1639	1.0704	1.0629	1.0974	1.0858
22	1.1957	1.1708	1.0944	1.0923	1.1100	1.1044
23	1.2157	1.1841	1.0775	1.0701	1.1072	1.0962
24	1.2288	1.1883	1.0684	1.0621	1.0925	1.0834
25	1.1945	1.1534	1.0731	1.0650	1.0999	1.0870
26	1.2075	1.1481	1.0694	1.0630	1.0938	1.0840
27	1.1808	1.1430	1.0646	1.0585	1.0839	1.0744
28	1.2653	1.1946	1.0658	1.0598	1.0858	1.0663

TABLE A-14
SUMMARY OF 2DB EIGENVALUES FOR PHASE II CONFIGURATIONS CALCULATED USING 10-GROUP CROSS SECTIONS WITH FULL-RANGE HETEROGENEITY FACTORS FROM DTFX AND TWOTRAN

Cell Radius (cm)	Mockup B_4C Rods Installed	Dry Core: No CH_2 Ingress		8.8 g/ℓ Channel CH_2	17.5 g/ℓ Channel CH_2	
		DTFX Cell Factors	TWOTRAN Cell Factors	DTFX Cell Factors	DTFX Cell Factors	TWOTRAN Cell Factors
54.79	None	0.97739	--	0.98050	0.98420	--
55.84	None	--	--	--	0.99128	--
56.10	None	--	--	0.98953	--	--
56.10	Center	--	--	0.98434	--	--
56.23	None	0.98762	0.98836	(0.9904)[a]	0.99384	0.99438
56.23	Center	0.98271	0.98343	(0.9852)[a]	0.98842	0.98883
56.23	Center Plus Ring[b]	0.96811	0.96872	--	0.97232	0.97220
56.62	None	--	--	0.99300	--	--
56.89	None	0.99204	--	--	--	--
59.38	Center Plus Ring[b]	0.98872	--	0.98977	--	0.99180

[a] Interpolation between results at 56.10- and 56.62-cm core radii.

[b] Ring of seven rods smeared over 42-drawer area at average radius of 38.90 cm.

TABLE A-15
SUMMARY OF 2DB EIGENVALUES FOR PHASE II CONFIGURATIONS CALCULATED USING 28-GROUP CROSS SECTIONS WITH FULL RANGE DTFX HETEROGENEITY FACTORS

Core Radius (cm)	Mockup B_4C Rods Installed	Dry Core No CH_2 Ingress	4.4 g/ℓ - Average Channel CH_2 Flooding		8.8 g/ℓ - Average Channel CH_2 Flooding		17.5 g/ℓ Channel CH_2 Flooding
			Smeared CH_2 Cell Factors	Lumped CH_2 Cell Factors	Smeared CH_2 Cell Factors	Lumped CH_2 Cell Factors	
54.79	None	0.97893	0.97933	0.97966	0.98076	0.98093	0.98450
56.10	None	--	--	--	--	0.98993	--
56.10	Center	--	--	--	--	0.98479	--
56.23	None	0.98913	--	--	0.99064	0.99080	0.99414
56.23	Center	0.98423	--	--	0.98548	0.98568	0.98879
56.23	Center Plus Ring	0.96949	--	--	--	--	0.97277
56.62	None	--	--	--	--	0.99340	--
56.89	None	0.99356	--	--	--	--	--
59.38	Center Plus Ring	0.99010	--	--	0.98998	0.99032	0.99223

TABLE A-16
DELAYED-NEUTRON PARAMETERS DERIVED FOR ANALYSES OF PHASE II GCFR ASSEMBLY WITH AND WITHOUT SIMULATED STEAM INGRESS

		Effective Delayed-Neutron Fraction (%Δk/k)			
		Dry Configuration		17.5 g/ℓ Channel CH_2	
Delay Group No.	Average Decay Constant (sec^{-1})	10-Group Analysis	28-Group Analysis	10-Group Analysis	28-Group Analysis
1	0.0130	0.00839	0.00828	0.00852	0.00844
2	0.0314	0.07406	0.07391	0.07420	0.07400
3	0.136	0.06393	0.06302	0.06451	0.06386
4	0.346	0.12389	0.12230	0.12447	0.12327
5	1.37	0.05689	0.05613	0.05695	0.05640
6	3.79	0.01855	0.01830	0.01853	0.01835
Total β-Effective (%Δk/k)		0.34571	0.34194	0.34718	0.34432
Generation Time (10^{-8} sec)		35.75	36.53	44.85	53.38
Conversions					
Ih/% Δk/k		937.0	943.2	931.8	936.9
Ih/$		323.9	322.5	323.5	322.6